ELSEVIER

Coordination Chemistry Reviews
150 (1996) 77–110

COORDINATION CHEMISTRY REVIEWS

Chapter 3
Relaxation

Contents

3.1. Introduction

In paramagnetic molecules, the magnetic nucleus does not see an unpaired electron as localized, but as spin density distributed throughout space, with an integrated intensity equal to that of a single electron. As a result, in every unit volume, the spin density corresponds to just a small fraction of an electron. Such a fraction will spend some time in the low Zeeman energy level(s) (negative M_S, see Chapter 1) and some time (slightly less) in the upper energy level(s) (positive M_S). Changes in M_S values involve changes in the orientation of the electron magnetic moment. The time sharing of the levels occurs through electron relaxation. Electron relaxation thus provides fluctuating magnetic fields and causes nuclear relaxation. When reference is made to spin density at the resonating nucleus, nuclear relaxation is contact in origin. The remaining spin density on the molecule and the relative electron relaxation are sensed by the resonating nucleus through dipolar coupling. The consequent nuclear relaxation is dipolar in origin. Often, reference is made to metal-centered relaxation; in this case, the whole electron is considered localized on the metal. Dipolar relaxation due to spin density elsewhere is called ligand-centered relaxation. This will be

0010-8545/96/$32.00
PII S0010-8545(96)01243-X

discussed in Section 3.4.1. Restricting ourselves to metal-centered nuclear relaxation, the fluctuation of the electron dipolar field at the nucleus due to electron relaxation can be easily visualized as depicted in Fig. 3.1(A). We now want to mention other mechanisms, besides electron relaxation, which occur in solution and through which unpaired electrons cause nuclear relaxation. All of these mechanisms will be discussed in detail in this chapter.

(i) Rotation of the molecular frame causes the nucleus to see the electron in different positions (Fig. 3.1(B)). If the rotation is faster than the electron relaxation time, on the rotational time scale the nucleus sees the electron with the same M_S

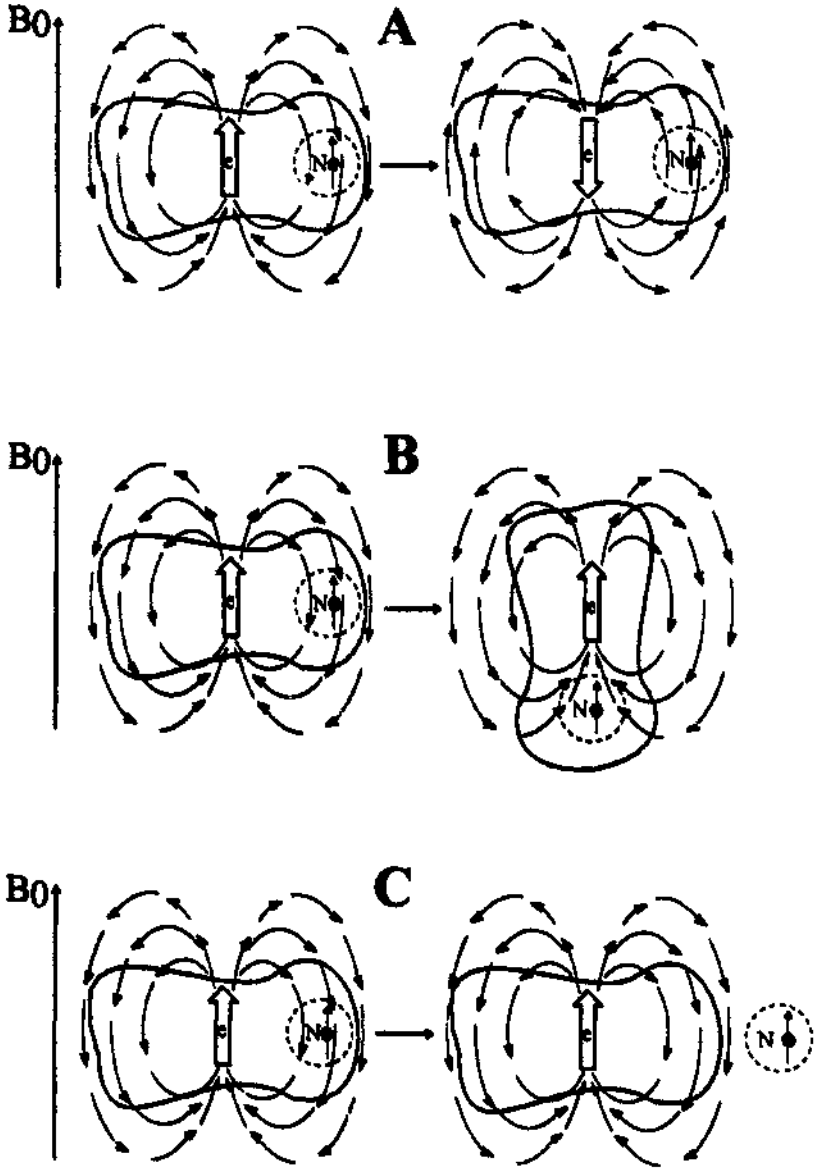

Fig. 3.1. Pictorial representation of the motions causing nuclear relaxation: electron spin relaxation (A), molecular rotation (B) and chemical exchange (C). It can be seen that the electron dipolar field at the nucleus fluctuates with time in direction (A), intensity (C) or both (B).

value but on different positions in space. This random motion of the electron around the nucleus is again seen as a fluctuating magnetic field that causes nuclear relaxation through dipolar coupling.

(ii) In addition, the nucleus sees the induced electronic magnetic moment $\langle\mu\rangle$ (Eq. (1.33)) which is aligned along the magnetic field as a result of the time average over the Zeeman levels. Upon rotation, the induced electronic magnetic field causes fluctuating magnetic fields sensed by the nucleus through space. This is another dipolar mechanism, that can be also visualized by referring to Fig. 3.1(B), related to the difference in electron population of the Zeeman levels and called Curie spin relaxation.

(iii) Finally, the approach and binding of a moiety containing the resonating nucleus to a group containing the unpaired electron, and the following detachment (chemical exchange), cause fluctuating magnetic fields at the nucleus (Fig. 3.1(C)) through both contact and dipolar mechanisms. A limiting case of chemical exchange is the outer sphere interaction (see Section 4.5).

Relaxation measurements provide a wealth of information both on the extent of the interaction between the resonating nuclei and the unpaired electrons, and on the time dependence of the parameters associated with the interaction. Whereas the dipolar coupling depends on the electron–nucleus distance, and therefore contains structural information, the contact contribution is related to the unpaired spin density on the various resonating nuclei and therefore to the topology (through chemical bonds) and the overall electronic structure of the molecule. The time-dependent phenomena associated with electron–nucleus interactions are related to the molecular system, and to the lifetimes of different chemical situations, for the resonating nucleus. Obtaining either structural or dynamic information, however, is only possible if an in-depth analysis of a series of experimental results provides sufficient data to characterize the system within the theoretical framework discussed in this chapter.

In real systems, each unpaired electron is delocalized through chemical bonds in the neighborhood of the metal, to an extent depending on the chemical properties of the system. Therefore, the dipolar interaction with the resonating nucleus should be evaluated by integrating over all the points where there is a finite unpaired spin density. Approximate procedures will be given in Section 3.4.1. An account of the nuclear relaxation times based on this general approach requires details of the electronic structure of the system, including the unpaired spin densities on the various non-s orbitals of the molecule, which is difficult to treat in general terms.

3.2. The correlation time

Electrons switch between levels characterized by M_S values. Let us examine now an ensemble of n molecules, each with an unpaired electron, in a magnetic field at a given temperature. The bulk system is at constant energy but at the molecular level electrons move, molecules rotate, there are concerted atomic motions (vibrations) within the molecules and, in solution, molecular collisions. Is it possible to have

information on these dynamics on a system which is at equilibrium? The answer is yes, through the *correlation function*. The correlation function is a product of the value of any time-dependent property at time zero with the value at time t, summed up to a large number n of particles. It is a function of time. In this case the property can be the M_S value of an unpaired electron and the particles are the molecules. The correlation function has its maximum value at $t=0$; since each molecule has one unpaired electron, the product of the M_S value at time zero times the M_S value at time t ($t=0$) is either $\frac{1}{2}\cdot\frac{1}{2}$ or $-\frac{1}{2}\cdot(-\frac{1}{2})$, i.e. always equal to $+\frac{1}{4}$. With time, some spins will change their orientation (Fig. 3.1(A)), so some particles will contribute by $-\frac{1}{4}$. The value of the correlation function $C(t)$ decreases. It can be shown that the decay of the correlation function can be approximated by an exponential in the absence of constraints (see Fig. 3.2)[1]

$$C(t)=\sum_i M_S(0)M_S(t)\approx\left(\sum_i \tfrac{1}{4}\right)\exp(-t/\tau_c) \tag{3.1}$$

From Eq. (3.1), the correlation time τ_c is defined as the time constant for which the correlation function exponentially decays to zero. At a time small compared with τ_c [$\exp(-t/\tau_c)\rightarrow 1$], we expect that essentially all spins maintain their original value. Therefore, most of the products will be $\frac{1}{4}$. At times long with respect to τ_c, we expect that all spins have changed their orientations many times, so that on the average half of the spins will result with the same M_S with respect to their original values, and the other half will have the other M_S value. Under these conditions, statistically half of the products will be $\frac{1}{4}$ and half $-\frac{1}{4}$, and the summation over a large number n of spins will yield zero.

Strictly speaking, the time dependence of $C(t)$ is not exponential for $t\ll\tau_c$; by referring to the above example, after a time much shorter than τ_c but still larger than zero, it is likely that $C(t)=C(0)$. Indeed, an expansion of the initial part of $C(t)$ would show a flat region around zero. In other words, it must be that $dC(0)/dt=0$, whereas for a true exponential $dC(0)/dt=1/4\tau_c$. Only for longer times does $C(t)$

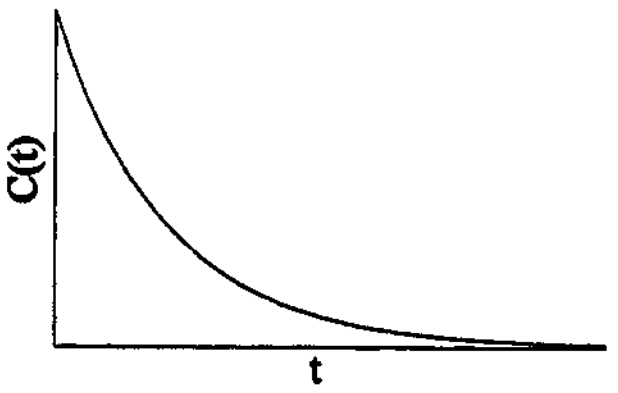

Fig. 3.2. Exponential decay with time of the correlation function.

[1] Here, and in the following, only positive values of time t are considered. Otherwise, all equations of the type of Eq. (3.1) should contain the absolute value of time in the exponential decay term, $\exp(-|t|/\tau_c)$.

become effectively exponential. The small initial deviation is, however, irrelevant for our purposes. Real cases of strong deviations from an exponential behavior do exist, but we will often restrict our interest to exponential correlation functions. In any case, the correlation time of a certain time-dependent process can be defined as the integral of the correlation function of that process, independently of the actual law for the time dependence.

The Fourier transform of an exponential decay in the time domain, as seen in Section 1.7.2, is a Lorentzian in the frequency domain:

$$J(\omega) = \frac{\tau_c}{1 + \omega^2 \tau_c^2} \tag{3.2}$$

This function (Fig. 3.3) has its inflection point at $|\omega|\tau_c = 1$. We say that the function undergoes a dispersion at $|\omega|\tau_c = 1$. This function provides the intensity of the various frequencies available in the lattice due to the fluctuations to which τ_c is related. It is also called noise, power, or spectral density function. The nucleus picks up the needed ω frequency for its relaxation. The probability of this to occur depends on the spectral density (i.e. on the value of function (3.2)) at that frequency.

Transverse nuclear relaxation can also occur when the local fields at the nucleus fluctuate slowly, i.e. with an ω frequency near zero (see also Section 3.4). Then the spectral density function will take the form

$$J(0) = \tau_c \tag{3.3}$$

This is a so-called non-dispersive term. Finally, in cases where two like nuclear spins relax each other, the 2ω frequency (double quantum transition) is needed besides ω,

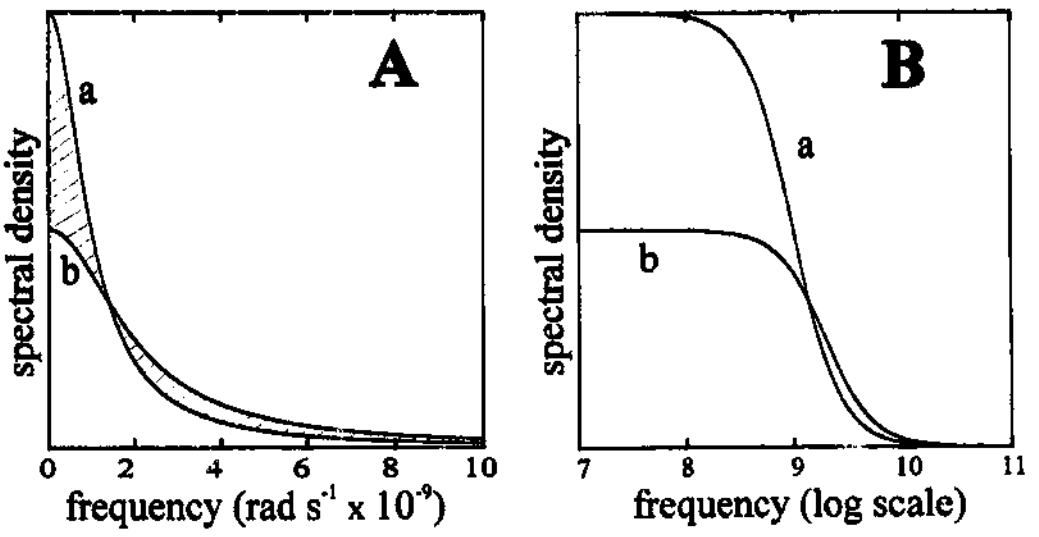

Fig. 3.3. Spectral density function $J(\omega)$ as a function of frequency, linear scale (A) and log scale (B). The profiles are obtained for $\tau_c = 1 \times 10^{-9}$ s (a) and 5×10^{-10} s (b). The two dashed areas in (A) are equivalent, showing that the area under the (a) and (b) curves is the same. The inflection points occur at $\omega\tau_c = 1$.

and then we will also have a function of the type

$$J(2\omega) = \frac{\tau_c}{1 + 4\omega^2\tau_c^2} \tag{3.4}$$

The present approach for nuclear relaxation can be extended to electron relaxation.

Once the correlation time is fixed, the value of the spectral density function at a given frequency can be determined, since all spectral density functions are normalized to unity. When τ_c is long, the spectral density is large in the small frequency range below τ_c^{-1}; when τ_c is short, we have a larger range of frequencies available but with a lower intensity (Fig. 3.3). Of course, τ_c refers to real physical mechanisms of fluctuations. We use the word fluctuation to indicate a movement which is random and unpredictable. We also use the words uncorrelated and stochastic for this behavior. The ω frequencies generally arise from sudden and short movements, which provide a range of frequencies just like in pulsed NMR (Section 1.7.2).

The movements capable of relaxing the nuclear spin that are of interest here are related to the presence of unpaired electrons, as has been discussed in Section 3.1. They are electron spin relaxation, molecular rotation, and chemical exchange. These correlation times are indicated as τ_s (electronic relaxation correlation time), τ_r (rotational correlation time), and τ_M (exchange correlation time). All of them can modulate the dipolar coupling energy and therefore can cause nuclear relaxation. Each of them contributes to the decay of the correlation function, which then decays according to the product

$$\exp(-t/\tau_s)\exp(-t/\tau_r)\exp(-t/\tau_M) = \exp[-(\tau_s^{-1} + \tau_r^{-1} + \tau_M^{-1})t]$$

Therefore, the overall correlation time is such that

$$(\tau_c^{-1})^{dip} = \tau_s^{-1} + \tau_r^{-1} + \tau_M^{-1} \tag{3.5}$$

i.e. its reciprocal is the sum of the single reciprocal correlation times. It often happens that only one dominates. In the case of relaxation by contact or isotropic coupling, only chemical exchange and electron relaxation can modulate the coupling. Thus

$$(\tau_c^{-1})^{con} = \tau_s^{-1} + \tau_M^{-1} \tag{3.6}$$

Sometimes distinction can be made between τ_{c1} and τ_{c2} if τ_s is specified as τ_{s1} (longitudinal) or τ_{s2} (transverse) electronic correlation time (see Section 3.4).

Electronic relaxation times fall in the range 10^{-7} to 10^{-13} s (Fig. 3.4), whereas the exchange time can be indefinitely long or as short as 10^{-10} s, depending on the

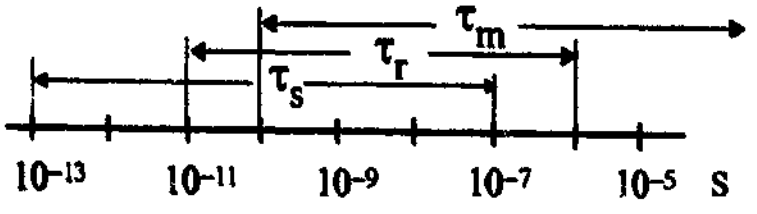

Fig. 3.4. Ranges of typical values for τ_s, τ_r and τ_M as defined in Eq. (3.5).

chemical bond strength. As far as rotation is concerned, the rotational correlation time can be predicted for spherical rigid particles [1–3].

$$\tau_r = \frac{4\pi\eta a^3}{3kT} = \frac{\eta MW}{dN_A kT} \tag{3.7}$$

where η is the viscosity (kg s^{-1} m^{-1}) of the solvent, a is the radius of the molecule, assumed spherical, MW is the molecular weight, (kg mol^{-1}), d is the density (kg m^{-3}) of the molecule (usually taken equal to 10^3), and N_A is Avogadro's constant. Values for τ_r in water solutions at room temperature range from 3×10^{-11} s for hexaaqua metal complexes, to 10^{-8} s for small proteins ($MW \approx 10$ kg mol^{-1}) to 10^{-6} s for larger macromolecules ($MW \approx 10^3$ kg mol^{-1}) (Fig. 3.4). The value of τ_r may also be estimated from T_1 measured at several magnetic fields on a diamagnetic analog of the metal complexes of interest. In fact, in diamagnetic systems the nuclear relaxation times are usually determined by dipolar coupling with other nuclei in the same molecule, the correlation time for the interaction being the rotational correlation time of the molecule itself (in the absence of chemical exchange).

3.3. Electron relaxation

From the foregoing discussion it appears that electron relaxation may be important for NMR on paramagnetic substances because τ_s may be the correlation time. Indeed, it is always important. Let us say we have two paramagnetic ($S = \frac{1}{2}$) compounds in water, one with τ_s of 10^{-8} s and the other with τ_s of 10^{-12} s. The size of each molecule is the same and such that the rotational correlation time is 10^{-10} s. For the former complex $\tau_c \approx \tau_r = 10^{-10}$ s and for the latter $\tau_c \approx \tau_s = 10^{-12}$ s. So, in one case nuclear relaxation depends on a correlation time which is due to rotation, whereas in the other it depends on the electron relaxation time. When the rotational mechanism determines the correlation time, and the latter happens to be long, nuclear relaxation rates will be invariably large and the NMR lines broad. As a consequence, we lose resolution and the capability of revealing connectivities among signals.

As will be seen soon, as a practical consequence, we can state that high resolution NMR can be fruitfully attempted for those systems for which τ_c is determined by τ_r: the shorter τ_s, the better. Detection of signals and exploitation of the NMR experiment is still convenient for diamagnetic moieties interacting with paramagnetic systems with long τ_s when in the presence of fast chemical exchange. Under these circumstances the linewidths of nuclei of the moiety which is in molar excess and exchanging with the moiety bound to the paramagnetic center are reduced by the molar fraction of the bound moiety, and still contain structural and dynamic information (see Chapter 4).

In Table 3.1 estimates of the electronic relaxation times at NMR field values are reported for some paramagnetic metal ions in solution and at room temperature. As τ_s values may be strongly field dependent, the low field limiting values τ_{s0}, when available, are also reported. The table also reports the calculated linewidth at

Table 3.1
Electronic relaxation times of some common paramagnetic metal ions and relative line broadening effects. Metal ions suitable for high resolution NMR are underlined

Metal ion	Electronic configuration	S	τ_S (s)	Reference	Line broadening[a] (Hz)
$\underline{Ti^{3+}}$	d^1	$\frac{1}{2}$	10^{-10}–10^{-11}	[4,5]	20–200
VO^{2+}	d^1	$\frac{1}{2}$	$\sim 10^{-8}$ [b]	[6–8]	10000
$\underline{V^{3+}}$	d^2	1	$\sim 10^{-11}$	[10,11]	50
V^{2+}	d^3	$\frac{3}{2}$	$\sim 10^{-9}$	[12–14]	5000
Cr^{3+}	d^3	$\frac{3}{2}$	5×10^{-9}–5×10^{-10}	[15–17]	3000–25000
$\underline{Cr^{2+}}$	d^4	2	10^{-11}–10^{-12}	est. from [18]	20–150
$\underline{Mn^{3+}}$	d^4	2	10^{-10}–10^{-11} [c]	[11,17,19]	150–1500
Mn^{2+}	d^5	$\frac{5}{2}$	$\sim 10^{-8}$ [d]	[16,21]	100000
Fe^{3+} (H.S.)	d^5	$\frac{5}{2}$	10^{-9}–10^{-11} [e]	[17,24,25]	200–12000
$\underline{Fe^{3+}}$ (L.S.)	d^5	$\frac{1}{2}$	10^{-11}–10^{-13}	[27,28]	0.5–20
Fe^{2+} (H.S.)	d^6, 5–6 coord.	2	10^{-12}–10^{-13}	[29,30], est. from [31]	5–20
	d^6, 4 coord	2	$\sim 10^{-11}$	est. from [32]	150
Co^{2+} (H.S.)	d^7, 5–6 coord.	$\frac{3}{2}$	5×10^{-12}–10^{-13}	[33,34]	2–50
	d^7, 4 coord.	$\frac{3}{2}$	$\sim 10^{-11}$	[35]	100
Co^{2+} (L.S.)	d^7	$\frac{1}{2}$	10^{-9}–10^{-10}	[13]	200–1000
$\underline{Ni^{2+}}$	d^8, 5–6 coord.	1	$\sim 10^{-10}$ [f]	[36]	500
	d^8, 4 coord.	1	$\sim 10^{-12}$	[39,40]	5
Cu^{2+}	d^9	$\frac{1}{2}$	$(1–5) \times 10^{-9}$	[41]	1000–5000
Ru^{3+}	d^5	$\frac{5}{2}$	10^{-11}–10^{-12}	[11,42]	2–20
Re^{3+}	d^4	2	10^{-12}–10^{-13}	[43]	5–20
Gd^{3+}	f^7	$\frac{7}{2}$	10^{-8}–10^{-9} [g]	[44–48]	20000–200000
Ln^{3+}	f^n		10^{-12}–10^{-13}	[49–52]	1–100

[a] For a proton at 5 Å from the metal; 500 MHz ^{1}H resonance frequency; only dipolar relaxation, estimated from Eq. (3.14), with $\tau_c = \tau_s$. [b] Field dependence of τ_s with a τ_{s0} value of 5×10^{-10} s has also been reported [9]. [c] τ_s values in the 10^{-11}–10^{-12} s range have also been proposed [20]. [d] τ_s is strongly field dependent. τ_{s0} values of 10^{-9}–10^{-10} s have been reported [22,23]. [e] τ_s is field dependent, τ_{s0} values being highly variable and ranging from 10^{-9} [25] to less than 10^{-11} s [26]. [f] τ_s is strongly field dependent. τ_{s0} values of 10^{-11}–10^{-12} s have been reported [37,38]. [g] τ_s is field dependent. τ_{s0} values of 10^{-8}–4×10^{-10} s have been reported [46,47].

500 MHz of a proton at 5 Å distance (in the presence of dipolar coupling, see later) for the case where τ_s is the correlation time. The underlined metal ions are those for which high resolution NMR is feasible and 2D NMR can be attempted also for nuclei experiencing hyperfine shifts. In particular, lanthanides(III) (except gadolinium(III)) and low spin iron(III) are particularly suitable for NMR. Then, tetrahedral nickel(II) and high spin six-coordinated cobalt(II) complexes have short electronic relaxation times. Manganese(III), low spin cobalt(II) and high spin heme-containing iron(III) compounds are at the borderline. Oxovanadium(IV), chromium(III), copper(II), manganese(II) and gadolinium(III) are not suitable for NMR experiments, except on nuclei in rapid exchange with diamagnetic species in excess. In Chapter 5 we will see that magnetic coupling in polymetallic systems may provide short effective electronic relaxation times independently of the electronic

relaxation times of the monometallic system. We are now going to cursorily review the principles of electron relaxation in order to be able to account for the values of the electronic relaxation times or to predict them.

3.3.1. The main mechanisms for electron relaxation

Mechanisms analogous to those illustrated in Fig. 3.1 apply also to electron relaxation. However, electrons have other more efficient relaxation mechanisms which overcome the former ones. Several possible mechanisms for electron relaxation have been successfully identified, and equations have been derived for many of them [53,54].

Solid-state theories ascribe electron relaxation to the coupling of electronic spin transitions with transitions between lattice vibrational levels, or more generally with *phonons*. Disappearance (depopulation of a vibrational level) or creation (population of a vibrational level) of phonons modulate the orbital component of the electron magnetic moment.

The orbit–lattice interaction allows the electron to change energy level, which may imply changes in the electron spin. It is customary to separate the coupling into direct processes [55], Orbach processes [56], and Raman processes [55,56], all of which are shown in Fig. 3.5. In the direct process, a phonon with the same energy as the electron spin transition is required. The direct process may be important

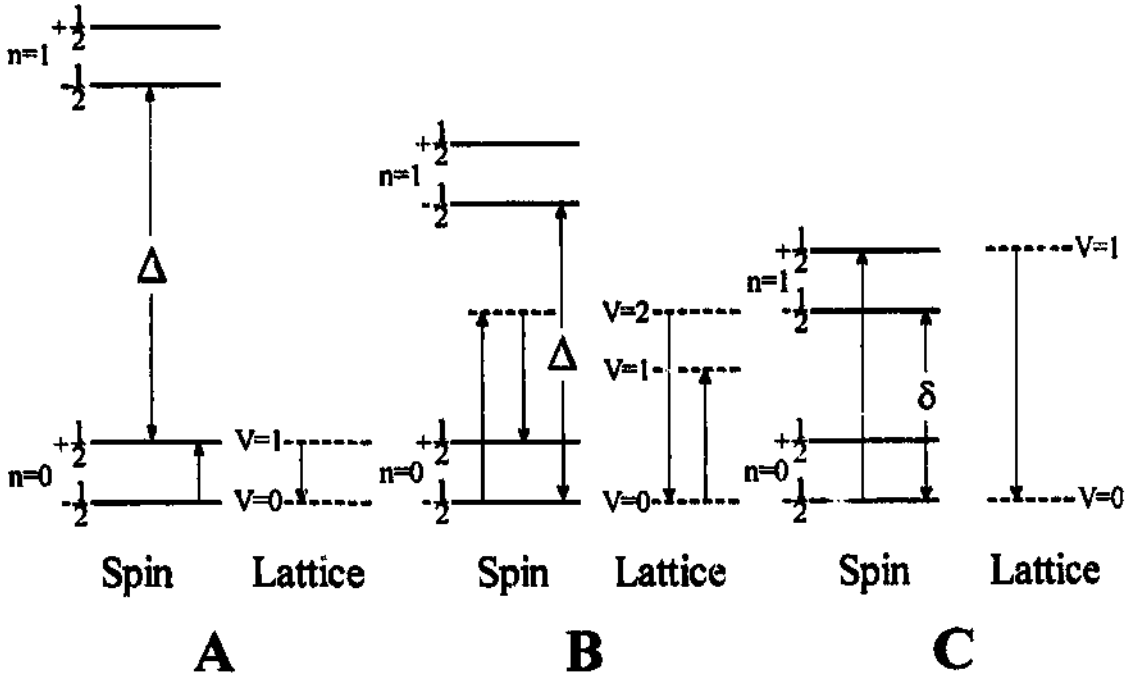

Fig. 3.5. Lattice and spin transitions are coupled by (A) direct processes, (B) Raman processes, (C) Orbach processes. The proximity of the excited electronic state favors both Orbach and Raman processes. The electronic states are labeled with n, the lattice vibrational states are labeled with V. Δ and δ indicate energy separations with excited states coupled to the ground state by spin–orbit coupling.

only at about liquid helium temperature, where only low energy phonons are available. The Orbach process requires low-lying electronic energy levels at about the energy of the phonons. At 300 K, corresponding to a thermal energy of about 200 cm^{-1}, the most probable phonon energies range between 50 and 1000 cm^{-1}. So, the electron–phonon coupling can provide the energy for jumps from the ground to the excited states and vice versa. Such jumps may involve spin changes. The Raman process is operative when there are not enough phonons available for electronic transitions which are too small in energy. Therefore, in the Raman process two phonons of high energy may simultaneously interact with the spin system so that their energy difference equals the electron Zeeman energy. This phenomenon can also be regarded as the scattering of a single phonon upon collision with the electron. The Orbach process provides the fastest mechanism. The Raman process may successfully compete when there are low-lying excited levels.

Following the solid-state approach, equations have been derived [57,58] also for the electron spin relaxation of $S=\frac{1}{2}$ ions in solution determined by the aforementioned processes. Instead of phonons, collisions with solvent should be taken into consideration, whose correlation time is usually in the range 10^{-11} to 10^{-12} s.

Two other mechanisms proposed for $S=\frac{1}{2}$ ions are typical of solutions and are determined by the rotation of the molecule. The first is due to the anisotropy of g and of A, and is proportional to τ_r. If g or A are anisotropic, their values are orientation dependent, and are therefore modulated by rotation [59]. The second is the so-called spin–rotation mechanism [60]. This mechanism arises from the fact that, upon a sudden change in the rotational motion of a molecule, for example after a collision, the molecular skeleton and the electron cloud may be slightly misplaced from one another, thus providing an instantaneous electric dipole moment. Therefore, there is a coupling between the spin angular momentum and the magnetic field generated by the instantaneous electric dipole moment, the latter related to the rotational angular momentum of the molecule; this coupling causes relaxation. The smaller the molecule, the larger the effect; for macromolecules, this mechanism is indeed negligible. The contribution to the relaxation rate of this mechanism is thus inversely proportional to that of the mechanisms modulated by τ_r, which increases with the size of the molecule. The effect is also proportional to the departure of $\bar{g}$ from g_e.

Additional relaxation mechanisms, for ions with $S>\frac{1}{2}$, arise from modulation of the quadratic ZFS in solution; these mechanisms have been discussed in detail by Bloembergen and Morgan [61] and Rubinstein et al. [16]. Deformations of the coordination polyhedron by collision with solvent molecules causes a transient ZFS which allows the coupling of rotation with spin transitions. The following equations have been derived for R_{1e} and R_{2e} for $S=1$

$$R_{1e}=\frac{2\Delta^2}{50}[4S(S+1)-3]\left(\frac{\tau_v}{1+\omega_s^2\tau_v^2}+\frac{4\tau_v}{1+4\omega_s^2\tau_v^2}\right) \tag{3.8}$$

$$R_{2e}=\frac{\Delta^2}{50}[4S(S+1)-3]\left(3\tau_v+\frac{5\tau_v}{1+\omega_s^2\tau_v^2}+\frac{2\tau_v}{1+4\omega_s^2\tau_v^2}\right) \tag{3.9}$$

here Δ^2 is the mean squared fluctuation of the ZFS and τ_v is the correlation time for the instantaneous distortions of the metal coordination polyhedron. Analogous equations also hold for the two electronic transitions $\frac{1}{2} \rightarrow -\frac{1}{2}$ and $\frac{1}{2} \rightarrow \frac{3}{2}$ of $S = \frac{3}{2}$ systems [16]. For $S = \frac{5}{2}$ three different relaxation times for each type should be considered [16]. Eqs. (3.8) and (3.9) are still good approximations for their effective averages. From Eqs. (3.8) and (3.9), the low-field limiting value of the electronic relaxation rate τ_{s0}^{-1} is given by $\tau_{s0}^{-1} = (\Delta^2/5)\,[4S(S+1) - 3]\tau_v$.

From the foregoing, the importance of the contribution of the various electronic relaxation mechanisms can be considered qualitatively for various cases. The least efficient mechanisms are the rotational mechanisms (g, A modulation) and spin rotation, which account for R_{1e} values up to $10^9\ s^{-1}$ and are only detected in the absence of other mechanisms. Contributions from the modulation of the quadratic ZFS to the relaxation rates through solvent bombardment can range from 10^8 to $10^{11}\ s^{-1}$, depending on the extent of the instantaneous geometrical distortions and spin–orbit coupling. It should be remembered that the extent of the splitting of an S manifold depends on the spin–orbit coupling constant, which increases from left to right and from top to bottom in the periodic table. A new mechanism based on a generalization of the spin rotation mechanism, and which is valid when the spin–orbit coupling energy is larger than the energy separation from the first excited electronic state, has been proposed which accounts for electron relaxation rates as large as $10^{11}\ s^{-1}$, e.g. for low spin ruthenium(III) complexes [62,63]. The Orbach and Raman processes may be the only processes that can account for relaxation rates higher than $10^{11}\ s^{-1}$. Although in solution there are no phonons, something similar is required to allow for fast electron relaxation. The Orbach process occurs when there are energy separations between ground and excited states in the range $100–1000\ cm^{-1}$.

$S = \frac{1}{2}$ ions like Cu^{2+} have no ZFS, small magnetic anisotropy and, in general, excited states far above the ground state in energy. Electronic relaxation times are therefore long. The main relaxation mechanism operative for copper(II) complexes is probably the Raman process [64] in the solid state. In solution, besides a Raman-type relaxation mechanism [64], contributions from modulation of g and A anisotropy by molecular tumbling may also be operative for small complexes. Symmetric copper complexes are known to experience dynamic Jahn–Teller effects. In the case of six-coordinated complexes elongation occurs along the three principal axes (Fig. 3.6). The occurrence of elongation is random with a correlation time of about 5×10^{-12} s. Elongation changes the hyperfine coupling constant between the copper nucleus and the unpaired electrons. This can be a further electron relaxation mechanism operative for example for the $Cu(OH_2)_6^{2+}$ complex [65–67]. $S = \frac{1}{2}$ ions like low spin iron(III), with ground levels deriving from an orbitally degenerate ground level in cubic symmetry (Fig. 3.7), may have low-lying excited states; therefore, Orbach processes are likely to be very efficient and short relaxation times are expected. The same holds for pseudooctahedral cobalt(II) and pseudotetrahedral nickel(II) chromophores. $S = \frac{5}{2}$ ions, like high spin manganese(II) and high spin iron(III), have small g anisotropy and first excited levels much higher than the ground level, since they arise from a different free ion term. In these cases, modulation of the quadratic

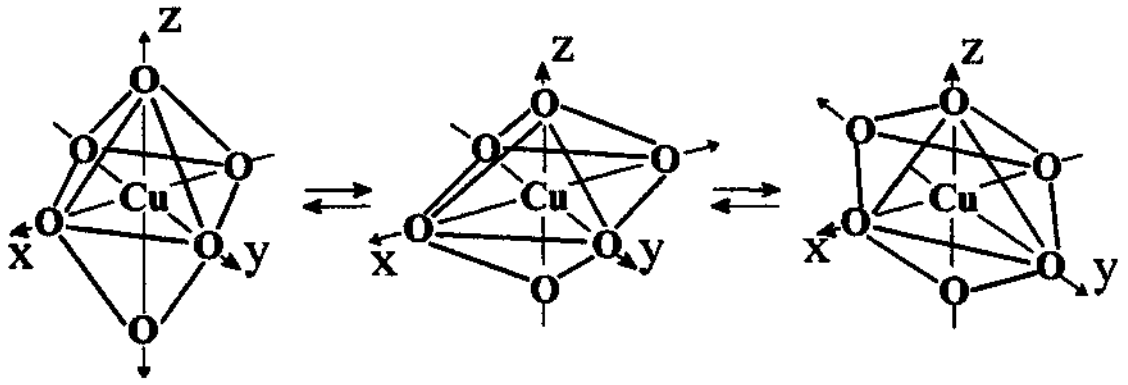

Fig. 3.6. Elongations along the three principal axes of the Cu–O bonds in the hexaaqua copper(II) complex due to dynamic Jahn–Teller effects occur randomly with a correlation time of about 5×10^{-12} s.

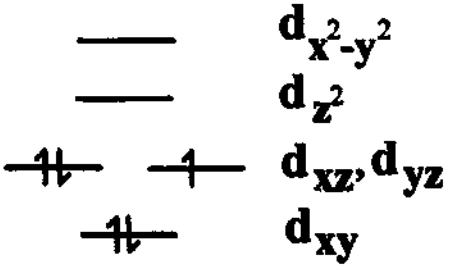

Fig. 3.7. A typical low symmetry splitting of the orbitally degenerate $^2T_2$ ground state of low spin iron(III).

ZFS is probably the most efficient relaxation mechanism in solution; such a mechanism is much more efficient for iron(III) than for manganese(II), since in the former spin–orbit coupling is larger and the first excited state is closer. Pseudooctahedral nickel(II) and pseudotetrahedral cobalt(II) have excited states higher in energy than those in the pseudotetrahedral and pseudooctahedral analogs already discussed, so the Orbach and Raman relaxation mechanisms are expected to be relatively less efficient and probably comparable with the modulation of the quadratic ZFS. All lanthanide ions, with the exception of gadolinium(III), are likely to be relaxed by Orbach-type processes, although some very efficient Raman processes are also invoked on the basis of the temperature dependence [51,52]. For gadolinium(III), which has an ^8S free ion ground term, the modulation of the quadratic ZFS is again the dominant mechanism [44–48].

3.4. Nuclear relaxation due to dipolar coupling with unpaired electrons

From the classic description of the coupling between two point dipoles with magnetic moments μ_1 and μ_2, the energy of the interaction E^{dip} is proportional to their scalar product and to the inverse of the third power of their distance (Eq. (1.1)). If the reciprocal orientation of the two vectors changes randomly with time, the fluctuating magnetic field produced by one at the location of the other may induce

spin transitions on the other center, and thus provide a relaxation pathway. The interest here is limited to nuclear spin transitions induced by fluctuating magnetic fields originating from unpaired electron spins. It should be remembered that the electronic magnetic moment is orders of magnitude larger than that of nuclei; for example, the magnetic moment of the free electron is 658 times that of the proton (Section 1.2).

While keeping in mind the general picture of nuclear relaxation in paramagnetic systems as described in Section 3.1, it is appropriate to consider first the simple case of dipolar coupling between two point-dipoles as if the unpaired electrons were localized on the metal ion. The enhancement of the nuclear longitudinal relaxation rate R_{1M} due to dipolar coupling with unpaired electrons, is proportional to the average of the square of the interaction energy and to the appropriate spectral density functions[2]:

$$R_{1M} \propto \langle (E^{\mathrm{dip}})^2 \rangle f(\omega, \tau_c) \tag{3.10}$$

Consider a single electron and a single nucleus separated by a distance r in a magnetic field B_0, and whose interaction is only dipolar in origin. The energy levels of the coupled spin system in a magnetic field $\boldsymbol{B}_0$ are given by the usual Hamiltonians (1.14), (1.18) and (1.51):

$$\mathscr{H} = g_e \mu_B \boldsymbol{S} \cdot \boldsymbol{B}_0 - \hbar \gamma_I \boldsymbol{I} \cdot \boldsymbol{B}_0 + \boldsymbol{I} \cdot \boldsymbol{A} \cdot \boldsymbol{S} \tag{3.11}$$

where the first two terms refer to the Zeeman interactions for the electron and nucleus ($\hbar\gamma_I = g_I \mu_N$) respectively, and the $\boldsymbol{I} \cdot \boldsymbol{A} \cdot \boldsymbol{S}$ term is the dipolar coupling between the two (which averages zero in solution in the absence of magnetic anisotropy). The energy levels, the transition frequencies ω, and the relative transition probabilities per unit time W, are shown in Fig. 3.8. The nuclear longitudinal relaxation rate can be expressed in terms of the probabilities of the transitions involving nuclear spin flipping:

$$R_{1M} = \frac{1}{10}\left(\frac{\mu_0}{4\pi}\right)^2 \frac{\hbar^2 \gamma_I^2 \gamma_S^2}{r^6}\left[\frac{\tau_c}{1+(\omega_I - \omega_S)^2\tau_c^2} + \frac{3\tau_c}{1+\omega_I^2\tau_c^2} + \frac{6\tau_c}{1+(\omega_I+\omega_S)^2\tau_c^2}\right] \tag{3.12}$$

which is the Solomon equation [68]. The three terms in parentheses are proportional to the transition probabilities and contain the spectral density functions $f(\omega, \tau_c)$

[2] We recall here that the time average of the interaction energy E^{dip} between two point-dipoles is zero (Chapter 2), while the time average of its square is different from zero. The average dipolar shift in solution (pseudocontact shift) depends on the presence of magnetic anisotropy, which is necessary to give a non-zero average of E^{dip}; dipolar relaxation, on the contrary, will occur independently of the presence of magnetic anisotropy.

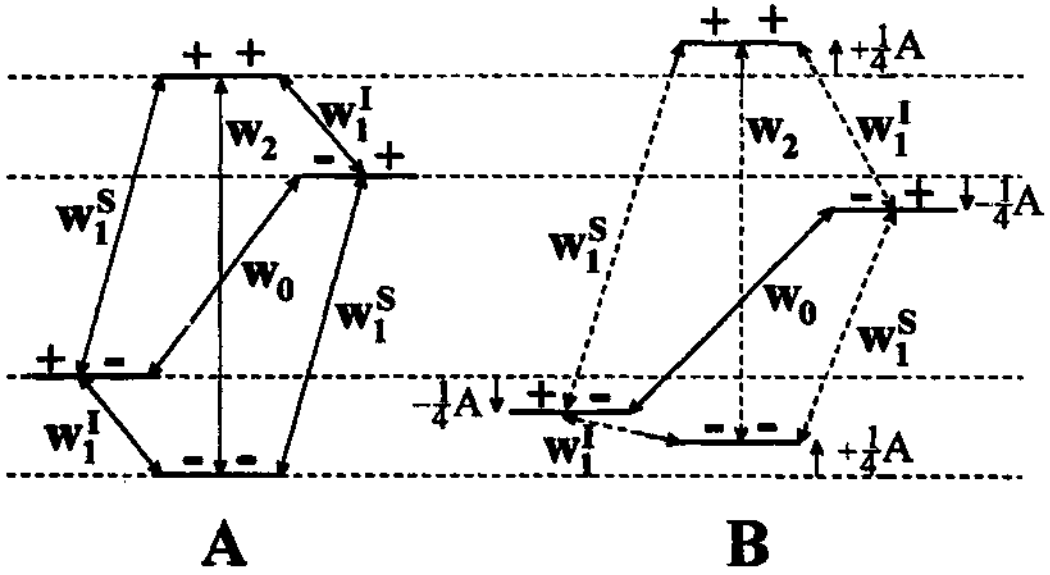

Fig. 3.8. Energy levels, transition frequencies and transition probabilities per unit time (W_0, W_1 and W_2) in a magnetically coupled two-spin system ((A) dipolar coupling; (B) contact coupling). A is the contact hyperfine coupling constant.

already discussed. The frequencies needed for the nuclear transitions are: ω_I, $\omega_I + \omega_S$ and $\omega_I - \omega_S$. This equation can be generalized [69,70] to systems with $S > \frac{1}{2}$.

$$R_{1M} = \frac{2}{15}\left(\frac{\mu_0}{4\pi}\right)^2 \frac{\gamma_I^2 g_e^2 \mu_B^2 S(S+1)}{r^6} \times \left[\frac{\tau_c}{1+(\omega_I-\omega_S)^2\tau_c^2} + \frac{3\tau_c}{1+\omega_I^2\tau_c^2} + \frac{6\tau_c}{1+(\omega_I+\omega_S)^2\tau_c^2}\right] \tag{3.13}$$

Note that Eq. (3.13) contains S but not I; R_{1M} is independent of I because it refers to $\Delta M_I = 1$ transitions [68,70]. J is needed instead of S for lanthanides. Analogously [68–70], an equation can be derived for R_{2M}:

$$R_{2M} = \frac{1}{15}\left(\frac{\mu_0}{4\pi}\right)^2 \frac{\gamma_I^2 g_e^2 \mu_B^2 S(S+1)}{r^6}\left[4\tau_c + \frac{\tau_c}{1+(\omega_I-\omega_S)^2\tau_c^2} + \frac{3\tau_c}{1+\omega_I^2\tau_c^2} + \frac{6\tau_c}{1+(\omega_I+\omega_S)^2\tau_c^2} + \frac{6\tau_c}{1+\omega_S^2\tau_c^2}\right] \tag{3.14}$$

R_{2M} differs from R_{1M} principally for the non-dispersive term. It is well known in NMR that frequencies near zero contribute to R_2 but not to R_1. When ω_S and ω_I are much smaller than τ_c^{-1} (fast motion limit) the denominators of the fractions between brackets become unity, and the Solomon Eqs. (3.13) and (3.14) reduce to

$$R_{1M} = R_{2M} = \frac{4}{3}\left(\frac{\mu_0}{4\pi}\right)^2 \frac{\gamma_I^2 g_e^2 \mu_B^2 S(S+1)}{r^6}\tau_c \tag{3.15}$$

At a magnetic field of 2.35 T the proton transition frequency (Larmor frequency)

is: $\nu_I = 100$ MHz; $|\omega_I| = 6.28 \times 10^8$ rad s^{-1}; $|\omega_S| = 4.13 \times 10^{11}$ rad s^{-1}. The ratio $|\omega_S|/|\omega_I|$ is 658 if the nucleus is a proton, and higher for other nuclei (except tritium, see Appendix I). Therefore, the values $|\omega_I \pm \omega_S|$ in Eqs. (3.13) and (3.14) can be approximated by $|\omega_S|$.

It should be recalled that the longitudinal relaxation process requires energy exchange with the lattice. In this case, the lattice is represented by the electron spin system, which exchanges energy with the nuclear spin system. As was pointed out in Section 1.7.1, every process that causes R_1 relaxation also contributes to R_2 relaxation. In the fast motion limit, the coupling with the lattice has the same effect on the magnetization along the z axis and on that in the xy plane, and $R_1 = R_2$. However, outside this limit the two functions $f_1(\omega, \tau_c)$ for R_{1M} and $\frac{1}{2}f_2(\omega, \tau_c)$ for R_{2M}, corresponding to the expressions in parentheses in Eqs. (3.13) and (3.14) diverge, leading to $R_{1M} < R_{2M}$. The function $f_1(\omega, \tau_c)$ has its maximum value when the rate constant τ_c^{-1} equals the nuclear Larmor precession frequency $|\omega_I|$ (Fig. 3.9), which makes the coupling of the electron and nuclear spins most efficient. The function $\frac{1}{2}f_2(\omega, \tau_c)$ increases monotonically with τ_c and differs from $f_1(\omega, \tau_c)$ for $\tau_c > |\omega_I|^{-1}$ (Fig. 3.9) because of the frequency-independent term $4\tau_c$.

R_{1M} and R_{2M} values also depend on the applied magnetic field, as ω_I and ω_S are determined by it ($|\omega_I| = \gamma_I B_0$; $|\omega_S| = \gamma_S B_0 = 658|\omega_I|$ for protons). The magnetic fields currently used range from that of the Earth to 18.8 T ($|\omega_I|/2\pi = 800$ MHz for protons). The field dependence of $f_1(\omega, \tau_c)$ (Fig. 3.10) shows two plateaus whose heights are in a 10/3 ratio and depend on the value of τ_c. The τ_c parameter is considered constant within the magnetic field range used, but this may not always be so (Section 3.3). The inflection point of the first dispersion is halfway between the two plateaus and corresponds to a magnetic field value at which $|\omega_S| = \tau_c^{-1}$; the

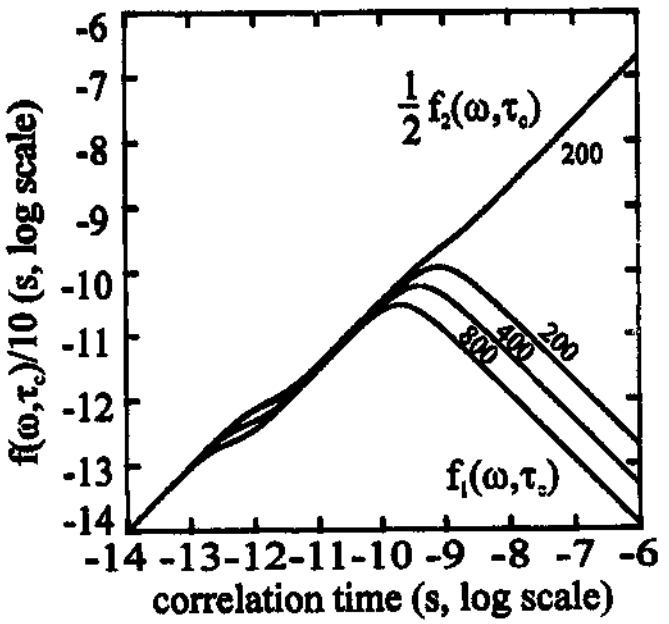

Fig. 3.9. Plot of $f_1(\omega, \tau_c)$ and $\frac{1}{2}f_2(\omega, \tau_c)$ of Eqs. (3.13) and (3.14) against τ_c for various proton Larmor frequencies (MHz).

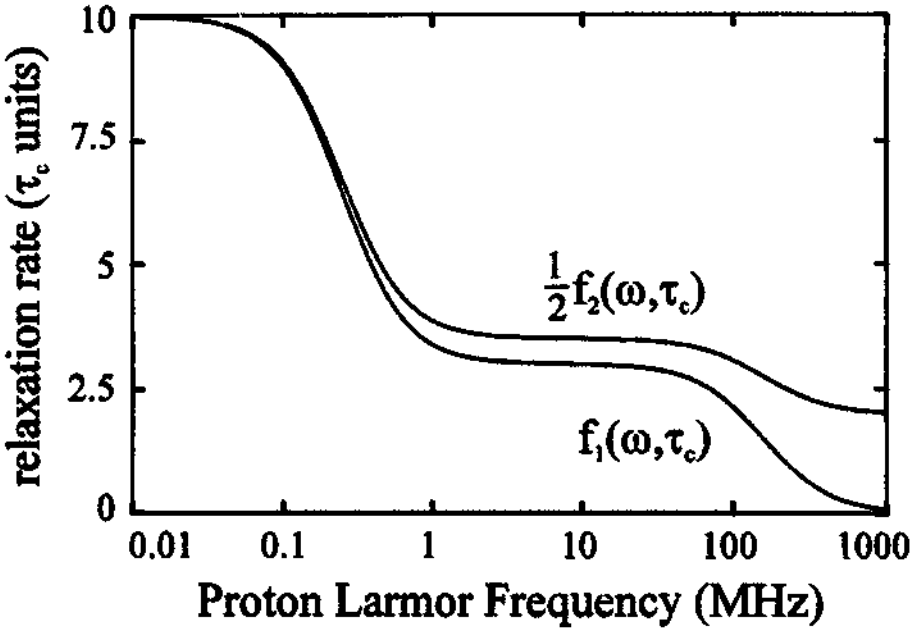

Fig. 3.10. Plot of $f_1(\omega, \tau_c)$ and $\frac{1}{2}f_2(\omega, \tau_c)$ of Eqs. (3.13) and (3.14) as a function of magnetic field (expressed as proton Larmor frequency; log scale). $\tau_c = 2 \times 10^{-9}$ s.

inflection point of the second dispersion is halfway between the second plateau and zero, and corresponds to $|\omega_I| = \tau_c^{-1}$.

The field dependence of $\frac{1}{2}f_2(\omega, \tau_c)$ is similar to that of $f_1(\omega, \tau_c)$ (Fig. 3.10), except that the relative height of the two plateaus is 20/7 and at high field the function levels off at a finite value that is one-fifth of the low field limit, because of the field independent term $4\tau_c$.

In the foregoing discussion, the electron–nucleus spin system was assumed to be rigidly held within a molecule isotropically rotating in solution. If the molecule cannot be treated as a sphere, its motion is, in general, anisotropic and three different correlation times should be considered. Furthermore, if the molecule is not rigid, the correlation times for rotations about single bonds should also be taken into account. For the case of a metal ion rigidly held to a macromolecule, but with a coordinated water molecule freely rotating about the M–O bond, the effect of neglecting the latter rotation on the calculation of R_{1M} for the protons is estimated to be about 20% [71]. The exact magnitude of the effect is a function of the angle that the metal–proton vector makes with the M–O bond.

When τ_c is significantly affected by τ_s, then it can be magnetic field dependent, since electron relaxation can often be described by equations similar to those for nuclear relaxation (see for example Eqs. (3.8) and (3.9)). Owing to this dependence, longitudinal (T_{1e}) and transverse (T_{2e}) electronic relaxation times may not be equal and, strictly speaking, when electron relaxation is the dominant correlation time, Eqs. (3.13) and (3.14) should be written as

$$R_{1M} = \frac{2}{15}\left(\frac{\mu_0}{4\pi}\right)^2 \frac{\gamma_I^2 g_e^2 \mu_B^2 S(S+1)}{r^6}\left(\frac{7\tau_{s2}}{1+\omega_S^2\tau_{s2}^2} + \frac{3\tau_{s1}}{1+\omega_I^2\tau_{s1}^2}\right) \tag{3.16}$$

$$R_{2M} = \frac{1}{15}\left(\frac{\mu_0}{4\pi}\right)^2 \frac{\gamma_I^2 g_e^2 \mu_B^2 S(S+1)}{r^6}\left(4\tau_{s1} + \frac{13\tau_{s2}}{1+\omega_S^2\tau_{s2}^2} + \frac{3\tau_{s1}}{1+\omega_I^2\tau_{s1}^2}\right) \tag{3.17}$$

where the terms containing ω_S, $\omega_I + \omega_S$ and $\omega_I - \omega_S$ have been collected for simplicity, since $|\omega_I| \ll |\omega_S|$. The longitudinal relaxation time $T_{1\rho}$ in the rotating frame is also shortened through coupling with unpaired electrons, according to the following equation [70]:

$$R_{1\rho M} = \frac{1}{15}\left(\frac{\mu_0}{4\pi}\right)^2 \frac{\gamma_I^2 g_e^2 \mu_B^2 S(S+1)}{r^6}\left(\frac{4\tau_{s1}}{1+\omega_1^2\tau_{s1}^2} + \frac{13\tau_{s2}}{1+\omega_S^2\tau_{s2}^2} + \frac{3\tau_{s1}}{1+\omega_I^2\tau_{s1}^2}\right) \tag{3.18}$$

It differs from the equation for R_{2M} for the substitution of the non-dispesive term with an $\omega_1\tau_s$ dependent term, where ω_1 is the nuclear Larmor frequency in the B_1 field. Since the latter frequency is always such that $|\omega_1|\tau_c \ll 1$, $R_{1\rho M}$ can be safely taken equal to R_{2M}. This also holds for the other nuclear relaxation mechanisms discussed in the following sections.

In the low field (or fast motion) limit, in the absence of chemical exchange, and for $T_{2e} = T_{1e}$, Eqs. (3.16)–(3.18) reduce to

$$R_{1M} = R_{2M} = R_{1\rho M} = \frac{4}{3}\left(\frac{\mu_0}{4\pi}\right)^2 \frac{\gamma_I^2 g_e^2 \mu_B^2 S(S+1)}{r^6} T_{1e} \tag{3.19}$$

justifying the qualitative statement that the shorter the electronic relaxation times the smaller the paramagnetic effects on nuclear relaxation.

3.4.1. Generalized dipolar coupling

As anticipated in Sections 2.2.2 and 3.1, the unpaired electrons should not be considered as point-dipoles centered on the metal ion. They are at the least delocalized over the atomic orbitals of the metal ion itself. The effect of the deviation from the point-dipole approximation under these conditions is estimated to be negligible for nuclei already 3–4 Å away [72]. Electron delocalization onto the ligands, however, may heavily affect the overall relaxation phenomena. In this case the experimental R_{iM} may be higher than expected, and the ratios between the R_{iM} values of different nuclei does not follow the sixth power of the ratios between metal to nucleus distances In the case of hexaaqua metal complexes the point-dipole approximation provides shorter distances than observed in the solid state (Table 3.2) for both ^{1}H and ^{17}O. This implies spin density delocalization on the oxygen atom. Ab initio calculations of R_{1M} have been performed for both ^{1}H and ^{17}O nuclei in a series of hexaaqua complexes (Table 3.2). The calculated metal nucleus distances in the assumption of a purely metal-centered dipolar relaxation mechanism are sizably smaller than the crystallographic values for ^{17}O, and the difference dramatically increases from $3d^5$ to $3d^9$ metal ions [73]. The differences for protons are quite smaller [73].

R_{1M} calculations in the presence of ligand-centered contributions are possible for metal complexes with ligands having dominant π spin density delocalization

Table 3.2
Crystallographic values of metal–hydrogen and metal–oxygen distances in hexaaqua complexes of divalent 3d metal ions[a] compared with calculated effective distances

Measurements	Metal ions				
	Mn	Fe	Co	Ni	Cu
^1H data					
r_{cryst} (pm)	290.6	290.6	278.1	275.5	270.4
r_{eff} (pm)	290.0	289.5	276.3	273.1	268.4
$r^6_{cryst} \cdot \langle 1/r^3 \rangle^2_{eff}$[b]	1.01	1.02	1.04	1.05	1.05
^{17}O data					
r_{cryst} (pm)	222.0	222.0	209.0	206.1	201.0
r_{eff} (pm)	219.8	211.7	190.5	174.9	172.3
$r^6_{cryst} \cdot \langle 1/r^3 \rangle^2_{eff}$[b]	1.06	1.33	1.74	2.67	2.52

[a] From Ref. [73]. M–H distances were calculated using $r_{O-H} = 95.7$ pm and HOH = 104.52. [b] The effective distances account for the experimental T_{1M}^{-1} by considering the electronic distribution predicted from ab initio MO calculations. $r^6_{cryst} \cdot \langle 1/r^3 \rangle^2_{eff}$ is the predicted enhancement coefficient of T_{1M}^{-1} with respect to a pure metal-centered dipolar relaxation mechanism.

mechanisms. With certain approximations, the relaxation rates of protons and carbon atoms in sp^2 CH moieties can be expressed [74–76] as the sum of a metal-centered term (given by the Solomon equation), a ligand-centered term and a cross term. The ligand-centered contributions will be proportional to the spin density ρ_{2p_z} in the carbon $2p_z$ orbital, and to the square of the reciprocal third power of the average nucleus $2p_z$ electron distance. In a particular case the following equation has been reported [76]:

$$R_{1M} = \frac{2}{15}\left(\frac{\mu_0}{4\pi}\right)^2 \gamma_I^2 g_e^2 \mu_B^2 S(S+1) \times \left[\rho_M^2 r_M^{-6} + \frac{4}{25}\rho_{2p_z}^2 \langle r_{2p_z}^{-3} \rangle^2 - \frac{2}{3}\rho_{2p_z}\langle r_{2p_z}^{-3}\rangle \rho_M r_M^{-3}\right] f_1(\omega, \tau_c) \qquad (3.20)$$

where $\langle r_{2p_z}^{-3} \rangle$ is calculated to be 5.3×10^{-7} pm^{-3} for protons and 3.2×10^{-6} pm^{-3} for carbon atoms [74,75]. In general, ρ_{2p_z} can be evaluated from the contact part of the proton hyperfine shift. This can be an easy-to-follow procedure for estimating ligand-centered contributions to the relaxation rates for π delocalized spin density [76].

3.5. Nuclear relaxation due to contact coupling with unpaired electrons

In the case of relaxation due to the contact term, the transition probabilities as defined in Fig. 3.8, where the splitting of the levels is now due to the contact

contribution, are found to be

$$W_{\omega_I} = W_{\omega_S} = W_{(\omega_S+\omega_I)} = 0 \tag{3.21}$$

This is because any scalar relaxation occurs through a flip-flop mechanism (Fig. 3.8).

$$W_{(\omega_S-\omega_I)} = \frac{1}{2}\left(\frac{A}{\hbar}\right)^2 \frac{\tau_c}{1+(\omega_S-\omega_I)^2\tau_c^2} \tag{3.22}$$

Here the correlation time is τ_c^{con} of Eq. (3.6). This differs from τ_c^{dip} of Eq. (3.5) because of the absence of the contribution from the rotational correlation time since the contact interaction, by its nature, is not altered by reorientation of the molecules. In the absence of chemical exchange phenomena ($\tau_M^{-1} \ll \tau_s^{-1}$), the correlation time equals the electronic relaxation time.

The enhancement of the longitudinal contact relaxation rate, after extension to the general case $S > \frac{1}{2}$, is given by the Bloembergen equation [70,77]

$$R_{1M} = \frac{2}{3}S(S+1)\left(\frac{A}{\hbar}\right)^2 \frac{T_{2e}}{1+\omega_S^2 T_{2e}^2} \tag{3.23}$$

where T_{2e} is the actual parameter determining τ_c. The equation for the transverse contact relaxation rate is [70,77]

$$R_{2M} = \frac{1}{3}S(S+1)\left(\frac{A}{\hbar}\right)^2 \left(T_{1e} + \frac{T_{2e}}{1+\omega_S^2 T_{2e}^2}\right) \tag{3.24}$$

The term $S(S+1)(A/\hbar)^2$ is proportional to the square of the coupling energy between

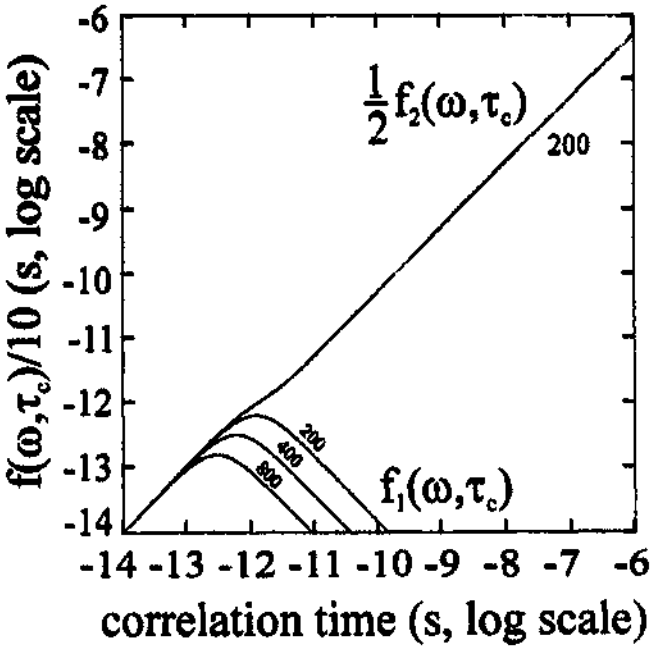

Fig. 3.11. Plot of $f_1(\omega, \tau_c)$ and $\frac{1}{2}f_2(\omega, \tau_c)$ of Eqs. (3.23) and (3.24) against τ_c for various proton Larmor frequencies (MHz).

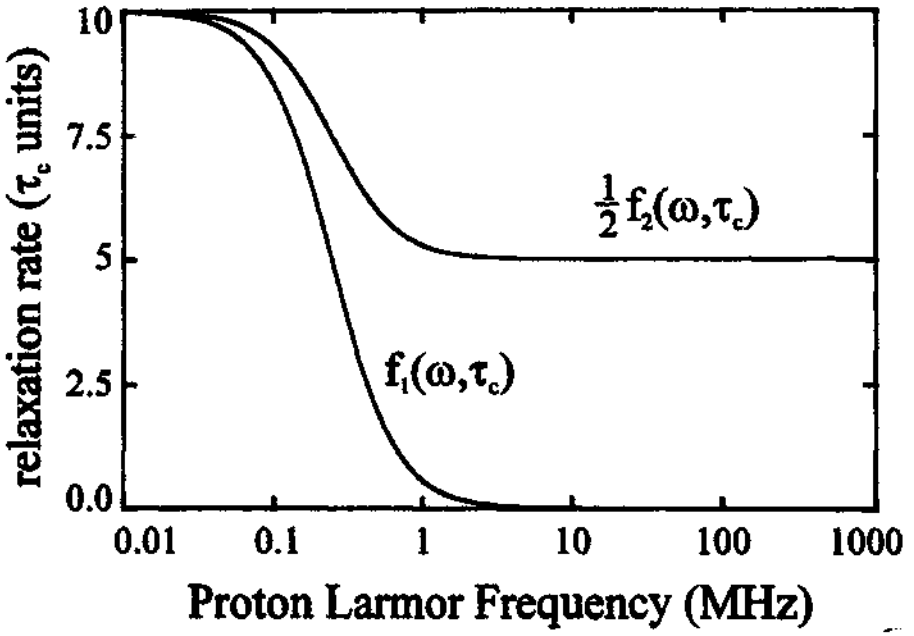

Fig. 3.12. Plot of $f_1(\omega, \tau_c)$ and $\frac{1}{2}f_2(\omega, \tau_c)$ of Eqs. (3.23) and (3.24) as a function of magnetic field (expressed as proton Larmor frequency; log scale). $\tau_c = 5 \times 10^{-11}$ s.

an electron spin vector S and the nuclear spin vector I. The same equations hold for lanthanides.

In the fast motion limit, and for $T_{1e} = T_{2e}$, Eqs. (3.23) and (3.24) reduce to

$$R_{1M} = R_{2M} = \frac{2}{3} S(S+1)\left(\frac{A}{\hbar}\right)^2 T_{1e} \tag{3.25}$$

As in the case of dipolar relaxation, the presence of a field-independent term in the equation for R_{2M} causes the two nuclear relaxation values to diverge for $\omega_S^2 T_{2e}^2 > 1$ (Figs. 3.11 and 3.12).

3.6. Curie nuclear spin relaxation

In deriving the dipolar and contact relaxation contributions due to the presence of unpaired electrons, as shown in Eqs. (3.16), (3.17), (3.23) and (3.24), the small difference in the population of the electron spin levels according to the Boltzmann distribution has been neglected. Such a difference accounts for the time-averaged magnetic moment of the molecule $\langle \mu \rangle$ (Eq. (1.33)), which is related to the $\langle S_z \rangle$ value defined in Eq. (1.31) for a simplified case. The interaction of the nuclear spins with this static magnetic moment related to $\langle S_z \rangle$ provides a further relaxation contribution. Such interaction, of course, cannot be modulated by electron relaxation since $\langle S_z \rangle$ is already an average over the electron spin states. The correlation time for the coupling is only determined by τ_r (or possibly by τ_M). This relaxation mechanism is usually called magnetic susceptibility relaxation or Curie spin relax-

ation — to reflect its relationship with the magnetic susceptibility of a sample (Curie law).

The dipolar contributions to R_{1M} and R_{2M} provided by this mechanism are [70,78,79]

$$R_{1M} = \frac{2}{5}\left(\frac{\mu_0}{4\pi}\right)^2 \frac{\gamma_I^2 g_e^2 \mu_B^2}{r^6} \langle S_z \rangle^2 \frac{3\tau_r}{1+\omega_I^2\tau_r^2}$$

$$= \frac{2}{5}\left(\frac{\mu_0}{4\pi}\right)^2 \frac{\omega_I^2 g_e^4 \mu_B^4 S^2(S+1)^2}{(3kT)^2 r^6} \frac{3\tau_r}{1+\omega_I^2\tau_r^2} \tag{3.26}$$

$$R_{2M} = \frac{1}{5}\left(\frac{\mu_0}{4\pi}\right)^2 \frac{\gamma_I^2 g_e^2 \mu_B^2}{r^6} \langle S_z \rangle^2 \left(4\tau_r + \frac{3\tau_r}{1+\omega_I^2\tau_r^2}\right)$$

$$= \frac{1}{5}\left(\frac{\mu_0}{4\pi}\right)^2 \frac{\omega_I^2 g_e^4 \mu_B^4 S^2(S+1)^2}{(3kT)^2 r^6} \left(4\tau_r + \frac{3\tau_r}{1+\omega_I^2\tau_r^2}\right) \tag{3.27}$$

In the case of lanthanides $\langle J_z \rangle^2$ should replace $\langle S_z \rangle^2$. Although the value of $\langle S_z \rangle^2$ is much smaller than the value of $S(S+1)/3$, which appears in the corresponding Solomon equations (Eqs. (3.16) and (3.17)), Curie spin relaxation may be significant when the dipolar coupling described by the Solomon equations is governed by the electronic relaxation times; that is, when the latter are much smaller than the rotational correlation times. Furthermore, since $\langle S_z \rangle^2$ depends on the square of the external magnetic field, Curie spin relaxation increases with the square of the nuclear Larmor frequency ω_I — see Eqs. (3.26) and (3.27) and Fig. 3.13. For example, when $\tau_r = 5 \times 10^{-11}$ s, $\tau_s = 5 \times 10^{-13}$ s and $B_0 = 14$ T, Curie spin relaxation can be sizably larger than the Solomon contribution to both R_1 and R_2. This is the case of aqualanthanide(III) ions except gadolinium(III) [49]. It is also quite common for Curie relaxation to dominate R_2 in macromolecules. For example, when $\tau_r = 10^{-7}$ s,

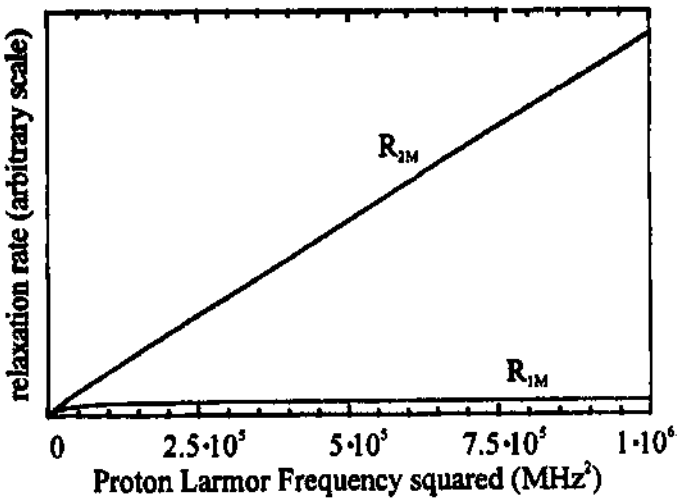

Fig. 3.13. Field dependence of the Curie spin relaxation contributions to R_{1M} and R_{2M} (arbitrary scale): $\tau_r = 2 \times 10^{-9}$ s.

$\tau_c = T_{1e} = 10^{-12}$ s, and $B_0 = 6$ T, Curie spin relaxation for R_{2M} is one order of magnitude larger than the Solomon contribution. Under these conditions Curie spin relaxation does not significantly contribute to R_{1M}; at high magnetic field ($\omega_I^2\tau_r^2 \gg 1$) the dependence on ω_I^2 in the numerator is canceled out. R_{1M} levels off at a value that is often small compared with the dipolar contribution.

The occurrence of this particular relaxation mechanism can be recognized through the field and temperature dependence of the linewidths. In the absence of other effects, the line broadening is proportional to the square of the magnetic field (Fig. 3.13) and to η/T^3, the latter dependence arising from the $1/T^2$ dependence of $\langle S_z\rangle^2$ (Eqs. (3.26) and (3.27)) and the η/T dependence of τ_r (Eq. (3.7)).

In principle, there may also be a Curie relaxation contribution of the contact-type whenever there is chemical exchange or intramolecular rotation to modulate the coupling. The contribution to R_{2M} would then be

$$R_{2M} = \frac{4}{3}\left(\frac{A}{\hbar}\right)^2 \langle S_z\rangle^2 \tau_M = \frac{4}{3}(\Delta\omega_I)^2\tau_M \tag{3.28}$$

where $\Delta\omega_I$ is the observed contact shift ($\Delta\omega_I = 2\pi\Delta\nu_I$).

3.7. The effect of g anisotropy and of the splitting of the S manifold at zero magnetic field

In the Solomon and Bloembergen equations for R_i ($i = 1, 2$) there is the ω_S parameter at the denominator of a Lorentzian function. Up to now ω_S has been taken equal to that of the free electron. However, in the presence of orbital contributions, the Zeeman splitting of the M_S levels changes its value and ω_S equals $|\gamma_S|B_0$ or $(g/\hbar)\mu_B B_0$. When g is anisotropic (see Fig. 1.16), the value of ω_S is different from that of the free electron and is orientation dependent. The principal consequence is that another parameter (at least) is needed, i.e. the θ angle between the metal-nucleus vector and the z direction of the g tensor (see Section 1.4). A second consequence is that the ω_S fluctuations in solution must be taken into account when integrating over all the orientations. Appropriate equations for nuclear relaxation have been derived for both the cases in which rotation is faster [80,81] or slower [82,83] than the electronic relaxation time. In practical cases, the deviations from the Solomon profile are within 10–20% (see for example Fig. 3.14).

When there is splitting of the S manifold at zero magnetic field, we should distinguish between half integer and integer S values. In the former case we always have an $M_S = -\frac{1}{2} \rightarrow \frac{1}{2}$ transition with energy of the order of $g\mu_B B_0$. The $M_S = \frac{1}{2} \rightarrow \frac{3}{2}$ transition, for example, may contain the term D (see for example Fig. 2.16). If D is much greater than the Zeeman energy, as is often the case, $|\omega_S|$ is much larger than in the case of the $-\frac{1}{2} \rightarrow \frac{1}{2}$ transition. Then the condition $|\omega_S|\tau_c \gg 1$ holds and the Lorentzian function has a negligible value. Such electronic transitions do not contribute to nuclear relaxation. It should also be mentioned that this holds when $D \gg \hbar\tau_c^{-1}$. Neglecting the ZFS may introduce an error of about a factor two in R_1.

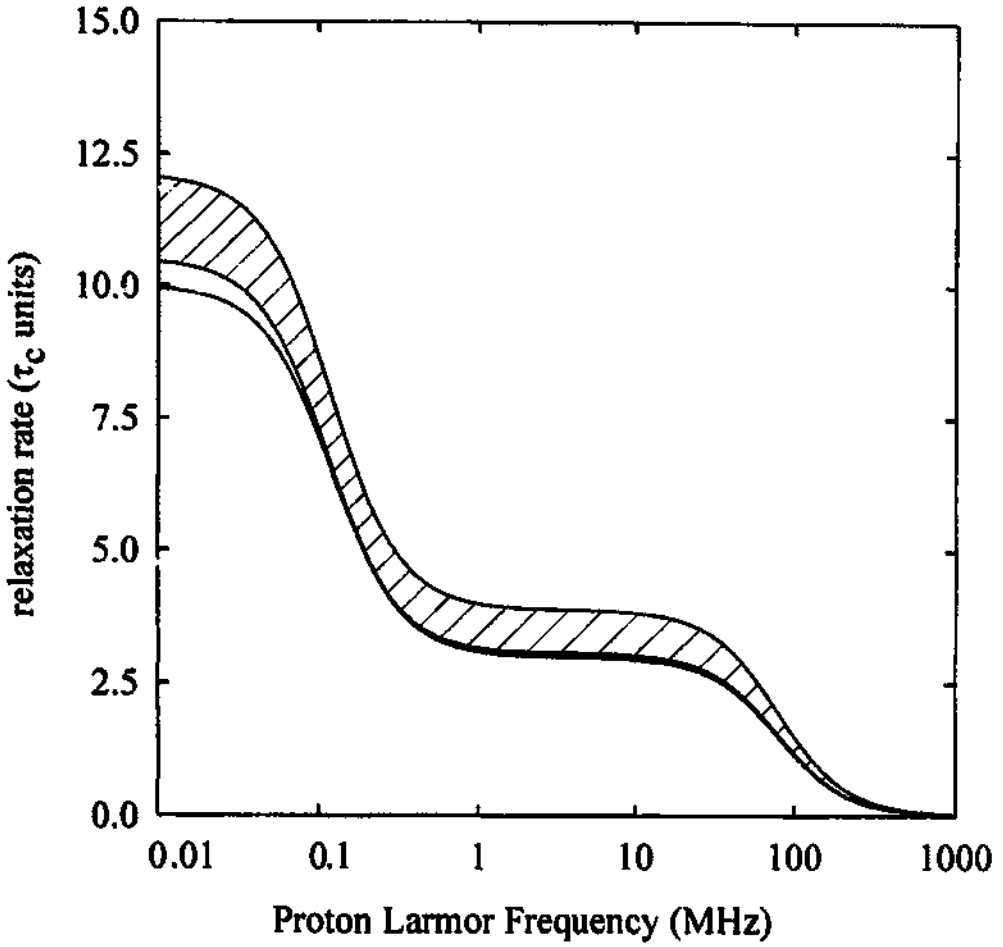

Fig. 3.14. Plot of the spectral density functions for dipolar relaxation in the presence of an axially symmetric g tensor. Conditions: $g_{\parallel} = 2.3$, $g_{\perp} = 2.0$, $\tau_c = 2 \times 10^{-9}$ s, $\theta = 0°$ (upper curve) and $\theta = 90°$ (middle curve) compared with the Solomon behavior (lower curve).

In the case of even S, all transitions contain D and it may happen that the term in ω_S never contributes to nuclear relaxation.

Another mechanism to provide splitting of the S manifold is the hyperfine coupling between the unpaired electron and the metal nucleus. For example, at zero magnetic field an $S = \frac{1}{2}$ $I = \frac{1}{2}$ system gives two sets of levels of degeneracy 3 and 1 separated by A (see Appendix II) where A is the metal-nucleus–unpaired-electron hyperfine coupling. The effect of this splitting is sizable, however, when $A > \hbar\tau_c^{-1}$ and at low magnetic fields where $A > g\mu_B B_0$. In high resolution NMR, the latter condition is practically never met.

A further effect of D and A when they influence nuclear relaxation is that again an angle is needed which takes into account the location of the resonating nucleus within the D (A) tensor frame. The theoretical approach to the description of R_1 under these circumstances gives approximate analytical solutions [35]. Numerical solutions are also available [84–86].

3.8. A comparison of dipolar, contact, and Curie nuclear spin relaxation

Once R_{1M} and R_{2M} have been measured, it is useful to try to understand the relative weight of dipolar, contact, and Curie spin contributions to the overall relaxation effect. Indeed, each of the three contributions is independently capable of providing valuable information whereas the whole value may not. The dipolar and Curie relaxation mechanisms — Eqs. (3.13), (3.14) and (3.27) — provide experimental values that are related to the distance of the nucleus from the paramagnetic metal and τ_c or τ_r, assuming that ligand-centered effects can be neglected. Measurements at various magnetic fields lead, in principle, to an estimation of these parameters. The field dependence of the dipolar contribution can be observed in any region of the accessible magnetic field range, that is from 0 to 800 MHz, whereas Curie relaxation can usually be observed only in the region above 100 MHz. Even at a single magnetic field value, measurements of dipolar R_{1M} contributions on various nuclei of the same moiety give information on their relative distance from the metal, as long as τ_c is the same. This is also true for R_{2M} values when they are determined by dipolar and/or Curie contributions.

The presence of contact relaxation indicates that a given moiety is covalently bound to a paramagnetic metal ion and provides an estimate of the absolute value of A (Eqs. (3.23) and (3.24)). Sometimes the contact coupling constant can be evaluated by chemical shift measurements, and it is therefore possible to predict whether the contact relaxation contributions to R_{1M}, R_{2M}, or both, are negligible or sizable.

Unlike hyperfine isotropic shifts, which often contain pseudocontact and contact contributions of the same order of magnitude, relaxation rates can often be recognized to be dominated by only one of the possible contributions. In addition, whereas contact and pseudocontact shifts may happen to have different signs, thereby making the factorization more uncertain, relaxation contributions are obviously always positive and additive.

Some qualitative guidelines can be given to make an a priori estimate of the relative weight of dipolar, contact, and Curie relaxation contributions. Consider first the fast motion limit where $R_{1M} = R_{2M}$ and none of the frequency-dependent terms is dispersed. The equations take the simple form already noted:

$$R_{1M} = R_{2M} = \frac{4}{3}\left(\frac{\mu_0}{4\pi}\right)^2 \frac{\gamma_I^2 g_e^2 \mu_B^2 S(S+1)}{r^6} \tau_c^{dip} + \frac{2}{3} S(S+1)\left(\frac{A}{\hbar}\right)^2 \tau_c^{con} \qquad (3.29)$$

Under these conditions the Curie spin contribution is always negligible (see Section 3.6). If $\tau_c^{dip} = \tau_c^{con}$ it is only necessary to compare the following two expressions:

$$\frac{4}{3}\frac{\gamma_I^2}{r^6} 8.6 \times 10^{-61} \quad \text{and} \quad \frac{2}{3}\left(\frac{A}{\hbar}\right)^2$$

where 8.6×10^{-61} is $(\mu_0/4\pi)^2 g_e^2 \mu_B^2$ ($T^2\,m^6$). For hydrogen nuclei, γ_I^2 is 7.16×10^{16} $rad^2\,s^{-2}\,T^{-2}$; whereas $(A/\hbar)^2$ does not usually exceed 10^{12} $rad^2\,s^{-2}$, and

is often found to be much lower. Thus, for metal-nucleus distances of 500 pm or smaller, the dipolar term is largely dominant. The value of the dipolar term drops dramatically with increasing r owing to its r^{-6} dependence, and for larger distances it could become smaller than the contact term. However, the $(A/\hbar)^2$ value is also qualitatively expected to decrease with increasing distance from the paramagnetic center. Therefore, unless some efficient unpaired spin delocalization pathway is operative, the dipolar term in proton relaxation is usually dominant for most systems of chemical interest.

The situation is different when the rotational correlation time is shorter than τ_s and therefore dominates the overall correlation time τ_c in the dipolar term. In this case, the relative importance of the dipolar term is decreased by a factor τ_s/τ_r, which can be as large as 10^2 to 10^3 for small complexes with rotational correlation times of 10^{-10} to 10^{-11} s and electronic relaxation times of 10^{-8} to 10^{-9} s — for example, Cu^{2+}, Mn^{2+}, and VO^{2+}. In macromolecular complexes, rotational correlation times are much larger, and situations of this type do not occur.

Outside the fast motion limit the relative weight of contact and dipolar interactions on R_{1M} and R_{2M} may also be different. The following considerations are particularly relevant to proton relaxation. Curie contributions to R_{2M} can be sizable. By comparing Eqs. (3.17) and (3.24) on the one hand and Eq. (3.27) on the other, it can be noted that they contain terms of the type

$$S(S+1)\tau_s \quad \text{and} \quad \omega_I^2 S^2 (S+1)^2 \tau_r$$

respectively. Therefore, it is expected that Curie contributions will be comparatively higher the higher the field, the higher S, and the higher the τ_r/τ_s ratio.

Once the Curie contribution to R_{2M} is estimated and factorized out, the contribution of contact and dipolar interactions can be estimated by examining the correlation time dependence of the paramagnetic relaxation depicted in Figs. 3.9 and 3.11. It appears that the maximum for R_{1M} occurs at $|\omega_I|\tau_c^{dip} \approx 1$ in the dipolar term and at $|\omega_S|\tau_c^{con} \approx 1$ in the contact term. Taking for simplicity $\tau_c^{dip} = \tau_c^{con}$, this means that in the intermediate situation where $|\omega_S|\tau_c^{dip} > 1 > |\omega_I|\tau_c^{con}$ the relative importance of the contact term is even smaller than that estimated in the fast motion limit. The equation for R_{2M} has non-dispersive terms in both the dipolar and contact contributions (accounting for one-fifth and one-half of the total effect measured in the fast motion limit respectively), and therefore the conclusions drawn in the fast motion limit are still qualitatively correct.

A comparison of R_{1M} and R_{2M} values may thus be useful to evaluate the occurrence of relaxation by contact interactions. Taking again $\tau_c^{dip} = \tau_c^{con} = \tau_c$, and keeping in mind the τ_c (or field) dependence of R_{1M} and R_{2M} as given by Eqs. (3.23) and (3.24), the R_{1M}/R_{2M} ratios are expected to be as reported in Table 3.3. When the estimate of τ_c is such that the intermediate situation ($|\omega_S|\tau_c > 1 > |\omega_I|\tau_c$) occurs, dominant dipolar relaxation will still give R_{1M}/R_{2M} ratios close to unity, whereas dominant contact relaxation will give $R_{2M} \gg R_{1M}$. In the latter case, no information is obtained concerning the mechanism controlling R_{1M}; however, an idea of what happens to R_{1M} can be perceived by the following procedure:

Table 3.3
Ratios between R_{1M} and R_{2M} for dipolar and contact contributions in the various motional regimes

	$\omega_s\tau_c < 1$	$\omega_s\tau_c > 1 > \omega_I\tau_s$	$\omega_I\tau_c > 1$
R_{1M}/R_{2M} (dipolar)	1	6/7	$\ll 1$
R_{1M}/R_{2M} (contact)	1	$\ll 1$	$\ll 1$

(1) use R_{2M} and a reasonable estimate for τ_c^{con} to calculate $(A/\hbar)^2$, as if R_{2M} were completely determined by contact relaxation;

(2) use the values of τ_c^{con} and $(A/\hbar)^2$ in the contact equation for R_{1M} to estimate the upper limit of the contact contribution of the longitudinal relaxation;

(3) compare this value with the experimental value of R_{1M} to check whether the contact contribution is negligible.

3.9. Nuclear parameters and relaxation

For nuclei other than protons, the magnetic moment is smaller (with the exception of ^{3}H). The nuclei with $I > \frac{1}{2}$ have a nuclear electric quadrupole moment which is an efficient source of nuclear relaxation by itself. Neglecting this contribution to relaxation, we may say that any dipolar coupling with the unpaired electron is smaller than in the case of the proton because the magnetic moment is smaller. Since the latter is proportional to γ_I and relaxation depends on the square of the coupling energy, R_i ($i = 1, 2$) depends on γ_I^2. As a consequence, the linewidth increase for, for example, ^{15}N nuclei due to dipolar interaction with unpaired electrons is 1/100 that of ^{1}H wher the two nuclei are at the same distance from the paramagnetic center. On the one hand, it is a pity that we soon lose such a wealth of information on the nucleus–electron coupling! On the other hand, this property can be exploited in the case of metal ions with slow electron relaxation, that cause broad ^{1}H lines. However, ^{2}H lines would be much sharper. ^{2}H NMR constitutes a common practice, for example, in small copper(II)-containing ligands. Of course, when the compounds are large in molecular size, quadrupolar relaxation becomes dominant and ^{2}H spectroscopy is not convenient or possible any longer.

As far as contact contributions are concerned, the nuclear γ_I parameter is contained in A (Eq. (2.2)) and therefore the same γ_I^2 dependence as in dipolar relaxation is introduced in contact relaxation. Again, heteronuclei are expected to be less relaxed owing to their smaller γ_I. However, heteronuclei can be directly coordinated to the paramagnetic metal ion. In this case the spin density on the nucleus can be very large and thus A can be very large compared with the proton case. Values of $(A/\hbar)^2$ as large as 10^{17} rad^2 s^{-2} can be obtained for directly coordinated nuclei like ^{17}O, ^{19}F, ^{14}N, and ^{15}N. In such cases, contact interaction may easily be the dominant mechanism for nuclear relaxation, especially for R_{2M}. In the case of imidazole complexes, even the non-coordinated nitrogen is quite broad. In this case, contact and/or ligand-centered effects provide efficient nuclear relaxation even for a nucleus at 4–4.5 Å from the metal [87].

3.10. The effect of temperature on the electron–nucleus spin interaction

No explicit temperature dependence is included in the equations for R_{1M} and R_{2M}, except for cases where Curie spin relaxation is the dominant term (Section 3.6). In the latter case, Curie paramagnetism has a T^{-1} dependence and therefore relaxation depends on T^{-2}. The effect of temperature on linewidths determined by Curie relaxation is dramatic also because of the τ_r dependence on temperature, as shown in Eq. (3.7). All the correlation times modulating the electron–nucleus coupling, either contact or dipolar, are generally temperature dependent, although in different ways, and their variation will therefore be reflected in the values of R_{1M} and R_{2M}.

In the limits of validity for the Solomon and Bloembergen equations, the correlation times for contact and dipolar relaxation are given by Eqs. (3.5) and (3.6) respectively. The exchange time τ_M is rarely short enough to dominate in Eqs. (3.5) and (3.6); however, when this is the case, a strong temperature dependence of the nuclear relaxation times is expected, because the variation of the exchange rate with temperature is generally exponential [88]. When the rotational correlation time is the dominant term, the effect of temperature would be anticipated to be less, since, as already seen, τ_r may be approximated by the Stokes–Einstein Eq. (3.7). The effect is enhanced, however, by the change in viscosity η of the solvent; in the case of water, η decreases as much as 2.7 times from 0 to 40 °C[3]. Qualitatively. Both τ_r and τ_M decrease with increasing temperature; this causes a decrease in the nuclear relaxation rates in the non-dispersive regions and an increase in the second half of the ω_I dispersive region (Fig. 3.15).

The temperature dependence of τ_s, including its sign, may be a matter of extensive speculation, mainly because the origin of the electron-spin relaxation mechanism in each particular case may be different, and in general is not known in detail. When equations of the type such as (3.8) and (3.9) hold, and by assuming that the correlation time for electron relaxation τ_v has an exponential temperature dependence, τ_s would be expected to increase with increasing temperature in the non-dispersive region ($|\omega_S|\tau_v \ll 1$) and to decrease in the dispersive region (high magnetic field). In fact, from Eqs. (3.8) and (3.9), τ_s^{-1} is proportional to $\tau_v/(1+\omega_S^2\tau_v^2)$, i.e. proportional to τ_v as long as $|\omega_s|\tau_v \ll 1$, and to τ_v^{-1} when $|\omega_s|\tau_v \gg 1$. However, this picture may be further complicated by a possible temperature dependence of the Δ^2 term in Eqs. (3.8) and (3.9), making it difficult to predict the overall behavior of τ_s. In addition, different electronic relaxation mechanisms may be operative at different temperatures, although the possibility that the switching from one mechanism to another occurs in a few tens of degrees around room temperature is rather unlikely.

In the coupled metal systems that will be discussed in Chapter 5, the effect of temperature is generally more complicated. Besides the effects described above, the overall temperature dependence will obviously also depend on the sign and magnitude of the exchange coupling constant J. The reader is referred to Chapter 5 for more details.

[3] The transport properties are also well modeled by exponential laws, but the energy is generally smaller than for chemical exchange.

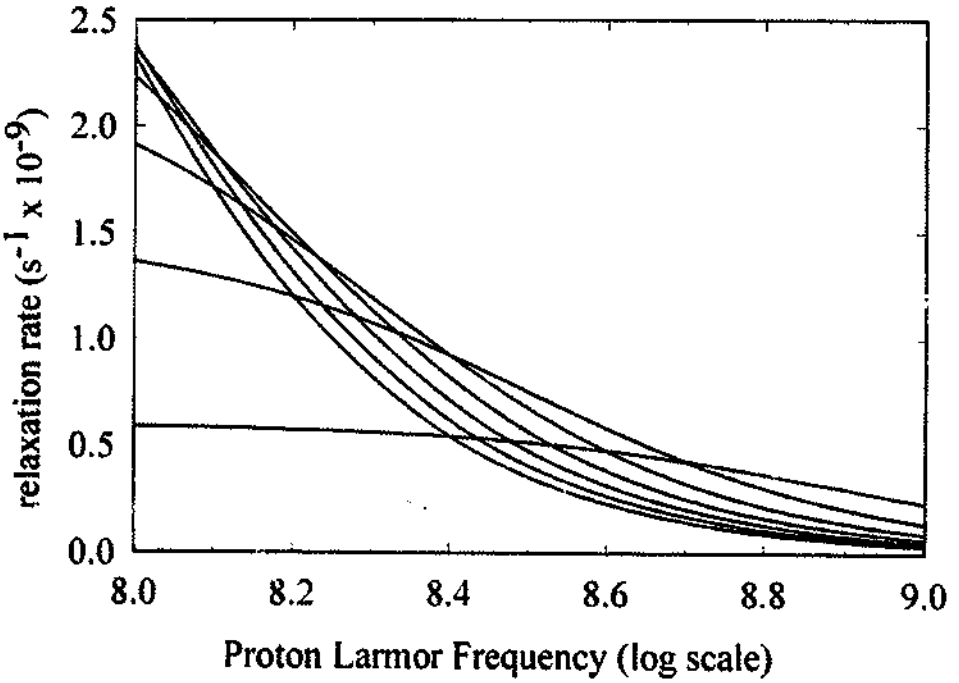

Fig. 3.15. Plot of $J_1(\omega, \tau_c)$ of Eq. (3.13) as a function of the proton Larmor frequency in the high frequency region. The curves are calculated for τ_c values decreasing from 2×10^{-9} s (upper curve on the left) in steps of 3×10^{-10} s.

The effects of chemical exchange on the NMR parameters, and hence the influence of temperature through modulation of the exchange process, will be considered in Section 4.3.

3.11. Stable free radicals

Free radicals have electronic relaxation times of about 10^{-7} s, which are the longest among paramagnetic compounds [53,54]. The correlation time for the NMR experiment when the radical is free in solution is the rotational correlation time.

Small molecules are already at the limit of detectability as far as proton NMR is concerned, whereas they are easily detected through ^{2}H NMR. If other factors concur favorably (interactions between radicals at high concentration, tendency to aggregate, availability of low-lying excited states), the proton NMR signals can also be detected for radicals. Nevertheless, it is, in general, a hard task to perform high resolution studies on radicals.

When the radical interacts rigidly with a macromolecule its rotational correlation time increases. For very large macromolecules, the correlation time for the NMR experiment eventually becomes the electronic relaxation time. If the bound radical still has motional freedom, this motion may be faster than the rotational time of the whole molecule and thus determine the correlation time. Of course, if the system is in chemical exchange, the exchange time may also be shorter than the electronic relaxation time and so represents the limiting NMR correlation time. An immobilized

radical produces a very large broadening effect on the NMR line of nearby nuclei, which is probably the largest effect that a paramagnetic species can cause[4].

3.12. NMR parameters and structural information

When a molecule is interacting with a metal ion without direct covalent bond there are no contact contributions nor ligand-centered effects to relaxation. This simplified case may occur in metalloproteins when a molecule occupies a protein pocket nearby the metal ion. The nuclear R_{1M} and R_{2M} can provide distances of the nuclei from the metal ion if the correlation time is known. However, in general this is an unknown[5]. Measurements at variable magnetic fields could be of help if we are lucky enough to be in one of the dispersion regions. Alternatively, substitution of protons with deuterons provides additional experimental data which permits the determination of the correlation time. If the pseudocontact shifts can be determined, we have a further hint to map the nuclei within the molecular frame (see Section 2.9). Finally, NOE or NOESY experiments (see Chapter 8) may provide further constraints to locate protons close to one another. In the early times of NMR, mapping procedures have been applied to small molecules binding to the metal in metalloproteins. In this case the results can be dramatically hampered by ligand-centered effects. These tend to make the experimental R_{1M} values close to one another, and they may then completely mislocate the molecule.

Several attempts to obtain structural information on molecules in solution have been made by using shift reagents (see Sections 2.8.5 and 2.9). In flexible molecules, many conformers may exist, the site of binding at the metal may be unknown, and the donor atoms may be more than one. As a result, the structural information should be analyzed with caution.

A safer procedure has been designed by using lanthanides at the calcium binding sites of proteins, that have essentially rigid structures. Lanthanides provide pseudocontact shifts which contain structural information. However, it is generally difficult to assign the signals without additional hints, for example from bidimensional spectroscopies. By using gadolinium, further information on the metal–proton distances can be obtained from nuclear relaxation.

Some attempts to obtain structural information by using spin labels as relaxation agents are possible. Again, it is difficult to proceed with the assignment, but if this is somehow obtained (see also Chapter 7), then R_{1M} and R_{2M} measurements provide distances, as the nuclear relaxation mechanism is dipolar in origin. Owing to the long correlation times, the effects on transverse relaxation are detectable on nuclei that are as far as 1.5 and 2 nm away from the paramagnetic probe. However, nuclei

[4] **Note added in proof**. This property has recently been used to obtain structural information on a radical–Pt–DNA moiety (S.U. Dunham and S.J. Lippard, J. Am. Chem. Soc., 107 (1995) 10702).

[5] **Note added in proof**. Recently a protocol has been suggested to use nuclear relaxation rates as structural constraints for the determination of solution structures of paramagnetic metalloproteins (I. Bertini, C. Luchinat and A. Rosato, Progr. Biophys. Mol. Biol., in press).

that are much closer may not be detectable because of the excessive line broadening. Therefore, radicals are best used as long-distance relaxation probes.

3.13. Experimental accessibility of nuclear relaxation parameters

As anticipated in Section 3.2, a nuclear longitudinal relaxation rate R_1 can be defined only when relaxation is an exponential process. This is at variance with nuclear transverse relaxation, which is always exponential and always defined by the transverse relaxation rate R_2. As far as longitudinal relaxation is concerned, when the return to the equilibrium value $M_z(\infty)$ of longitudinal nuclear magnetization after a 180° pulse is exponential, we can write (see Section 1.7.4)

$$M_z(t) = M_z(\infty) - 2M_z(\infty)\exp(-R_1 t) \tag{3.30}$$

If we consider that relaxation is further enhanced by interaction with a paramagnetic center, Eq. (3.30) becomes

$$\begin{aligned} M_z(t) &= M_z(\infty) - 2M_z(\infty)\exp(-R_1 t)\exp(-R_{1M} t) \\ &= M_z(\infty) - 2M_z(\infty)\exp[-(R_1 + R_{1M})t] \end{aligned} \tag{3.31}$$

The meaning of Eq. (3.31) is that any further decay function is multiplied by the original decay function if they are independent (see also Section 3.2). If both are exponential, then the whole process remains exponential and the rate constant is $R_{1\text{tot}} = R_1 + R_{1M}$. As already mentioned in Chapter 1, and as will be further explained in Chapter 6, longitudinal nuclear relaxation is often a non-exponential process. In our definition of R_1 (Section 1.7.4), it was assumed that all nuclei were independent of one another. In diamagnetic systems nuclei are often coupled to one another, influencing each other in such a way that one cannot be considered a lattice with infinite heat capacity for the other, and R_1 cannot be defined. Paramagnetic relaxation, however, is an exponential process within the broad range of validity of the equations given in this chapter. This is due to the fact that electrons have a much larger magnetic moment and relax so much faster than nuclei that they behave effectively as a lattice with infinite heat capacity. So, Eq. (3.31) takes the more general form

$$M_z(t) = M_z(\infty) - 2M_z(\infty)f(t)\exp(-R_{1M} t) \tag{3.32}$$

where $f(t)$ is a generic non-exponential decay accounting for diamagnetic interactions. In such a case, even if paramagnetic relaxation is exponential, R_{1M} cannot be easily extracted from the analysis of the overall decay. If paramagnetic relaxation is dominant, exponentiality is effectively imposed to the overall nuclear relaxation. If not, the detailed dependence of longitudinal nuclear magnetization as a function of time must be analyzed.

Experimental techniques are available to measure magnetization recovery under different conditions. These are, for instance, the selective and non-selective variants of the inversion recovery experiment described in Section 1.7.4, and will be discussed in more detail in Chapter 9. We anticipate here, from Chapters 6 and 9, in a qualitative way, the kind of information contained in these experiments.

In a non-selective inversion recovery experiment the 180° pulse inverts the magnetization of the nuclear spin under consideration as well as that of all other nuclear spins coupled to it. All spins will return to equilibrium and, simultaneously, will influence each other by, for example, dipolar coupling. In a selective experiment, only the nuclear spin under consideration is inverted by the pulse. During its return to equilibrium, it will also be influenced by dipolar coupling with the other, initially unperturbed spins. In both cases, diamagnetic relaxation mechanisms will superimpose to the exponential recovery due to the coupling with the paramagnetic center, and deviations from exponentiality will occur. These deviations will be, however, less severe for a non-selective experiment. Indeed, mutual influence between two nuclear spins I and J occurs through W_0 and W_2 terms (Chapter 6) analogous to the mutual influence between nuclear and electron spins I and S illustrated in Section 3.2 and Fig. 3.8. This influence will be maximal when $2\omega_I\tau_c \gg 1$, i.e. in the slow motion limit, where the W_2 terms become negligible. If we refer to the latter conditions, magnetization recovery of the inverted I spin in a selective experiment occurs by partially *decreasing* M_z of the neighbor spin J through magnetization transfer (Fig. 3.16). The presence of the neighbor thus "helps" the inverted spin to

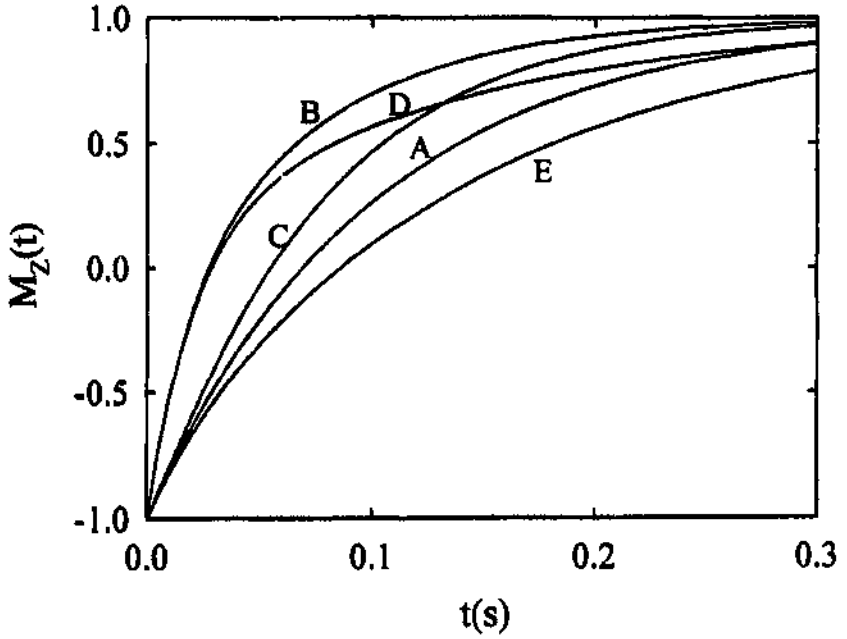

Fig. 3.16. Exponential recovery (A) of $M_z(t)$ of a nuclear spin I dipole coupled to a paramagnetic metal ion. When I is also coupled to another nuclear spin J, the latter also coupled to the metal ion, non-exponentiality occurs. If J relaxes faster than I, curves (B) and (C) are obtained for a selective and a non-selective experiment respectively. If J relaxes slower than I, curves (D) (selective) and (E) (non-selective) are obtained. If J relaxes at the same rate as I, a selective experiment gives an intermediate behavior between curves (B) and (D) (not shown), while a non-selective experiment gives pure exponential recovery (A). It is apparent that in all cases non-selective experiments perform better than selective experiments, as they are less sensitive to the non-exponentiality introduced by I–J coupling. Conditions: $R_{1M}^I = 10\,s^{-1}$; $R_{1M}^I = 20\,s^{-1}$ (B, C), $5\,s^{-1}$ (D, E) and $10\,s^{-1}$ (A). The I–J cross-relaxation rate σ_{IJ} (Chapter 6) is $-20\,s^{-1}$.

relax faster (curves (B) and (D)). This transfer of magnetization is maximal at $t = 0$, and becomes less effective with time (hence non-exponentiality arises). On the contary, in a non-selective experiment (curves (C) and (E)), the transfer of magnetization will be zero at $t = 0$, because both spins I and J are inverted. With time, transfer occurs from the slower relaxing to the faster relaxing spin: the slower will then relax slightly faster and the faster will relax slightly slower (again non-exponentiality occurs). If the two spins accidentally relax with the same rate, no net magnetization transfer occurs and recovery is again exponential. In any case, it is apparent that *R_{1M} values can always be better evaluated from non-selective rather than from selective experiments* because of this partial compensation effect, and particularly from the initial points of the decay when magnetization transfer is negligible. The stronger the I–J coupling, the worse the selective experiments perform with respect to non-selective ones. Although the underlying theory has been well known for many years, this simple rule has never been plainly formulated, even by specialists in the field. See also the note added in proof to Chapter 6 (i.e. footnote 1).

References

[1] G. Stokes, Trans. Cambridge Philos. Soc., 9 (1956) 5.
[2] A. Einstein, Investigations on the Theory of the Brownian Movement, Dover, New York, 1956, pp. 19–34.
[3] P. Debye, Polar Molecules, Dover, New York, 1929.
[4] R.C. Wilson and R.J. Myers, J. Chem. Phys., 64 (1976) 2208.
[5] I. Bertini, C. Luchinat and Z. Xia, Inorg. Chem., 31 (1992) 3152.
[6] D. Kivelson, J. Chem. Phys., 45 (1966) 1324.
[7] D.C. McCain and R.J. Myers, J. Phys. Chem., 71 (1967) 192.
[8] R.N. Rogers and G.E. Pake, J. Phys. Chem., 33 (1960) 1107.
[9] I. Bertini, C. Luchinat and Z. Xia, J. Magn. Reson., 99 (1992) 235.
[10] A.M. Chmelnick and D. Fiat, J. Magn. Reson., 8 (1972) 325.
[11] D.R. Eaton, J. Am. Chem. Soc., 87 (1965) 3097.
[12] G.L. McPherson, R.C. Koch and G.D. Stucky, J. Chem. Phys., 60 (1974) 1424.
[13] A. Bencini and D. Gatteschi, in G.A. Melson and B.N. Figgis (Eds.), Transition Metal Chemistry, Marcel Dekker, New York and Basel, 1982, pp. 1–178.
[14] B.A. Goodman and J.B. Raynor, in H.J. Emeleus and A.G. Sharpe (Eds.), Advances in Inorganic Chemistry and Radiochemistry, Academic Press, 1970.
[15] B.R. McGarvey, J. Phys. Chem., 61 (1957) 1232.
[16] M. Rubinstein, A. Baram and Z. Luz, Mol. Phys., 20 (1971) 67.
[17] G.N. La Mar and F.A. Walker, J. Am. Chem. Soc., 95 (1973) 6950.
[18] G.N. La Mar and G.R. Van Hecke, J. Am. Chem. Soc., 91 (1969) 3442.
[19] S.H. Koenig, R.D. Brown III and M. Spiller, Magn. Reson. Med., 4 (1987) 252.
[20] Z. Luz and D. Fiat, J. Chem. Phys., 46 (1967) 469.
[21] M. Grant, H.W. Dodgen and J.P. Hunt, Inorg. Chem., 10 (1971) 71.
[22] S.H. Koenig and R.D. Brown III, J. Magn. Reson., 61 (1985) 426.
[23] I. Bertini, F. Briganti, C. Luchinat and Z. Xia, J. Magn. Reson., 101 (1993) 198.
[24] I. Bertini, F. Capozzi, C. Luchinat and Z. Xia, J. Phys. Chem., 97 (1993) 1134.
[25] I. Bertini, O. Galas, C. Luchinat, L. Messori and G. Parigi, J. Phys. Chem., 99 (1995) 14217.
[26] J.B. Bloch and G. Navon, J. Inorg. Nucl. Chem., 42 (1980) 693.
[27] L.P. Yu, G.N. La Mar and K. Rajarathnam, J. Am. Chem. Soc., 112 (1990) 9527.
[28] L. Banci, I. Bertini, S. Marconi, R. Pierattelli and S.G. Sligar, J. Am. Chem. Soc., 116 (1994) 4866.

[29] Y. Ducommun, K.E. Newman and A. Merbach, Inorg. Chem., 19 (1980) 3696.
[30] Unpublished results from our laboratory, 1995.
[31] L. Banci, I. Bertini, S. Marconi and R. Pierattelli, Eur. J. Biochem., 215 (1993) 431.
[32] M.T. Werth, D.M. Kurtz Jr., I. Moura and J. LeGall, J. Am. Chem. Soc., 109 (1987) 273.
[33] A.M. Chmelnick and D. Fiat, J. Chem. Phys., 47 (1967) 3986.
[34] L. Banci, I. Bertini and C. Luchinat, Inorg. Chim. Acta, 100 (1985) 173.
[35] I. Bertini, C. Luchinat, M. Mancini and G. Spina, J. Magn. Reson., 59 (1984) 213.
[36] C. Chachaty, A. Forchioni, J. Verlet and J.C. Ronfard-Haret, Chem. Phys. Lett., 29 (1974) 436.
[37] H.L. Friedman, M. Holz and H.G. Hertz, J. Chem. Phys., 70 (1979) 3369.
[38] J. Kowalewski, T. Larsson and P.-O. Westlund, J. Magn. Reson., 74 (1987) 56.
[39] L.J. Ming, L. Banci, C. Luchinat, I. Bertini and J.S. Valentine, Inorg. Chem., 27 (1988) 4458.
[40] G.N. La Mar, J. Am. Chem. Soc., 87 (1965) 3567.
[41] L. Banci, I. Bertini and C. Luchinat, Magn. Reson. Rev., 11 (1986) 1.
[42] U.E. Steiner and D. Bürßner, Z. Phys. Chem. N.F., 169 (1990) 159.
[43] A. Paulo, A. Domingos, A. Pires di Matos, I. Santos, M.F.N.N. Carvalho and A.J.L. Pombiero, Inorg. Chem., 33 (1994) 4729.
[44] G.P. Vishnevskaya and B.M. Kozyrev, J. Struct. Chem., 7 (1966) 20.
[45] A. Hudson and J.W.E. Lewis, Trans. Faraday Soc., 66 (1970) 1297.
[46] S.H. Koenig, Magn. Reson. Med., 22 (1991) 183.
[47] G. Hernandez, M. Tweedle and R.G. Bryant, Inorg. Chem., 29 (1990) 5110.
[48] S. Aime, L. Barbero and M. Botta, Magn. Res. Imaging, 9 (1991) 843.
[49] I. Bertini, F. Capozzi, C. Luchinat, G. Nicastro and Z. Xia, J. Phys. Chem., 101 (1993) 198.
[50] S. Aime, M. Botta and G. Ermondi, Inorg. Chem., 31 (1992) 4291.
[51] S.K. Misra and U. Orhun, Solid State Commun., 63 (1987) 867.
[52] V.M. Malhotra, H.A. Buckmaster and J.M. Dixon, J. Phys. C, 13 (1980) 3921.
[53] I. Bertini, C. Luchinat and G. Martini, in C.P. Poole (Ed.), Handbook of Electron Spin Resonance, American Institute of Physics, New York, 1994, pp. 51–77.
[54] I. Bertini, C. Luchinat and G. Martini, in C.P. Poole (Ed.), Handbook of Electron Spin Resonance, American Institute of Physics, New York, 1994, pp. 79–310.
[55] J.H. Van Vleck, Phys. Rev., 57 (1940) 426.
[56] R. Orbach, Proc. R. Soc. London Ser. A: 264 (1961) 458.
[57] D. Kivelson, J. Chem. Phys., 33 (1960) 1094.
[58] S.A. Al'tshuler and K.A. Valiev, Sov. Phys. JETP, 35 (1959) 661.
[59] G.V. Bruno, J.K. Harrington and M.P. Eastman, J. Phys. Chem., 81 (1977) 11.
[60] P.W. Atkins and D. Kivelson, J. Chem. Phys., 44 (1966) 169.
[61] N. Bloembergen and L.O. Morgan, J. Chem. Phys., 34 (1961) 842.
[62] Yu.A. Serebrennikov and U.E. Steiner, J. Chem. Phys., 100 (1994) 7508.
[63] U.E. Steiner and Yu.A. Serebrennikov, J. Chem. Phys., 100 (1994) 7503.
[64] I. Bertini, C. Luchinat, R.D. Brown III and S.H. Koenig, J. Am. Chem. Soc., 111 (1989) 3532.
[65] D.H. Powell, L. Helm and A.E. Merbach, J. Chem. Phys., 95 (1991) 9258.
[66] J.H. Freed and R.G. Kooser, J. Chem. Phys., 49 (1968) 4715.
[67] R.G. Kooser, W.V. Volland and J.H Freed, J. Chem. Phys., 50 (1969) 5243.
[68] I. Solomon, Phys. Rev., 99 (1955) 559.
[69] A. Abragam, The Principles of Nuclear Magnetism, Oxford University Press, Oxford, 1961.
[70] S.H. Koenig, J. Magn. Reson., 47 (1982) 441.
[71] D.E. Woessner, J. Chem. Phys., 36 (1962) 1.
[72] R.M. Golding, R.O. Pascual and B.R. McGarvey, J. Magn. Reson., 46 (1982) 30.
[73] L. Nordenskiöld, L. Laaksonen and J. Kowalewski, J. Am. Chem. Soc., 104 (1982) 379.
[74] H.P.W. Gottlieb, M. Barfield and D.M. Doddrell, J. Chem. Phys., 67 (1977) 3785.
[75] D.M. Doddrell, P.C. Healy and M.R. Bendall, J. Magn. Reson., 29 (1978) 163.
[76] J. Mispelter, M. Momenteau and J.-M. Lhoste, J. Chem. Soc. Dalton Trans., (1981) 1729.
[77] N. Bloembergen, J. Chem. Phys., 27 (1957) 575.
[78] M. Guéron, J. Magn. Reson., 19 (1975) 58.
[79] A.J. Vega and D. Fiat, Mol. Phys., 31 (1976) 347.

[80] H. Sternlicht, J. Chem. Phys., 42 (1965) 2250.
[81] K.V. Vasavada and B.D. Nageswara Rao, J. Magn. Reson., 81 (1989) 275.
[82] I. Bertini, C. Luchinat and K.V. Vasavada, J. Magn. Reson., 89 (1990) 243.
[83] I. Bertini, F. Briganti, C. Luchinat, M. Mancini and G. Spina, J. Magn. Reson., 63 (1985) 41.
[84] L. Banci, I. Bertini, F. Briganti and C. Luchinat, J. Magn. Reson., 66 (1986) 58.
[85] R.R. Sharp, J. Chem. Phys., 98 (1993) 2507.
[86] I. Bertini, O. Galas, C. Luchinat and G. Parigi, J. Magn. Reson., 113 (1995) 151.
[87] Y. Yamamoto, N. Nanai, Y. Inoue and R. Chujo, J. Chem. Soc. Chem. Commun., (1989) 1419.
[88] F. Basolo and R.G. Pearson, Mechanisms of Inorganic Reactions. A Study of Metal Complexes in Solutions, Wiley, New York, 1963.